FOREWARD TO THE ORAL SESSION "GEOMATICS FOR EMERGENCY MANAGEMENT"

Piero Boccardo*

*Politecnico di Torino, Italy, piero.boccardo@polito.it

Disasters can be defined as "a serious disruption of the functioning of a community or a society involving widespread human, material, economic or environmental losses and impacts, which exceeds the ability of the affected community or society to cope using its own resources" (UNISDR 2009). Disasters can be classified according to the main causes, i.e. natural, technological or manmade disasters.

The effects of natural disasters on the environment and on the population can be understood by analyzing the relevant statistics over the past years, in terms of both economic and human losses. The information collected by the Centre for Research on the Epidemiology of Disasters (CRED) at the School of Public Health of the Université Catholique de Louvain located in Brussels, Belgium, and more specifically the data stored in the EM-DAT database (EM-DAT is a global database on natural and technological disasters that contains essential core data on the occurrence and effects of

more than 17,000 disasters in the world from 1900 to present) highlights (Guha-Sapir 2011) that in 2010 a total of 385 natural disasters were registered, with more than 297,000 casualties [Guha-Sapir et al., 2012]. Over 217 million people were affected worldwide and $123.9 billion of economic damages were estimated. Similar to the average over the last decade, hydrological disasters (events caused by deviations in the normal water cycle and/or overflow of bodies of water caused by wind setup, i.e. Flood and Mass Movement events) were by far the most numerous disasters in 2010, representing 56.1% of the total disaster occurrence in that year, and together with meteorological disasters - the second most frequent calamitous event – accounted for 79% of total occurrence.

Economic damages from natural disasters in 2010 were over 2.5 times higher than in 2009 ($47.6 billion), and increased by 25.3% compared to the annual average for the period 2000-2009 ($98.9 billion). From a geographical point of view, some 89% of all people affected by disasters in 2010 lived in Asia. Nevertheless, the European continent faced the biggest increase in disaster occurrence, whereas Asia had the largest decrease, counting fewer disasters, victims and damages compared to the last decade's annual averages.

Disaster Risk Reduction (DRR) activities are aimed to limit the impact of a disaster when it occurs, mainly by strengthening the community's capabilities to cope with a disaster, or to reduce the possibility of a disaster occurring. As clearly highlightedby the Disaster Risk Management (DRM) cycle, a general strategy commonly adopted to fulfill the aforementioned goal is based on an iterative cycle comprising the following phases:

Risk assessment, Mitigation and Prevention, Preparedness, Prediction and Warning, Response, and Recovery. Geomatics definitively plays a crucial role in the DRM cycle. Spatial Data Infrastructures (SDI) makes available global reference geospatial data and services that are transversally exploited in all the aforementioned DRM phases. Furthermore, the growing use of interoperable data formats based on international standards (e.g. Open Geospatial Consortium standards) make easier the integration of local geospatial datasets.

Early warning systems often rely on satellite remote sensing data to feed forecasting or nowcasting systems aimed "to generate and disseminate timely and meaningful warning information to enable individuals, communities and organizations threatened by a hazard to prepare and to act appropriately and in sufficient time to reduce the possibility of harm or loss" (United Nations 2009). Undoubtedly, data acquired by ground measuring stations are also involved in the process, but again the accurate georeferencing of such information is a crucial feature.

Adnan et Al. paper represents a good example of global early warning systems based on open source data such as Tropical Rainfall Measuring Mission (TRMM) Multi-satellite Precipitation Analysis (TMPA), the most commonly used data for detecting critical rainfall events.

This contribution presents the evaluation of TRMM monthly rainfall data (3B43) for Pakistan, using 15 years data from 1998 to 2012 in comparison to the ground rainfall data for the same period.

For calibration, regression analysis was performed for each month on the data of rain gauge stations and their corresponding pixel values from the satellite datasets. Regression equations were used to develop the calibrated seasonal and annual rainfall maps, as well as the monthly rainfall maps on district level.

From an operational point of view, recent major disasters (i.e. 2013 Philippines Typhoon, 2011 Italy earthquake, 2010 Haiti earthquake, 2010 Pakistan Flood and 2011 Japan tsunami) clearly demonstrated the potential role of geomatics in supporting emergency response and recovery. Remote sensing based analyses are nowadays frequently adopted to support both decision makers and responders in the field during disaster management activities, as recently clearly pointed out by the United Nations in the 2011 humanitarian appeal: "[…] Remote sensing in the hours and days after the Haiti earthquake yielded estimates of numbers of severely affected people that stood the test of time and allowed an unusually rapid flash appeal. [...] Similarly, in Pakistan, the plans in the revised flash appeal were mostly able to encompass the still expanding scale of needs thanks to information management using remote sensing and other resources necessary for a situation of limited ground access." (United Nations 2011. Section "Major natural disasters in 2010 and lesson learned").

Domeneghetti et Al. clearly highlights in his contribution the role of geomatics in an International cooperation framework as far as flood risk mitigation is concerned.

Based on the lesson learned after 2004 flood event in Haiti and Dominican Republic, the General Direction for Development and Cooperation of the Italian Department of Foreign Affairs funded through the Istituto Italo-Latino Americano (IILA, www.iila.org) an international cooperation initiative (ICI), coordinated and directed by the University of Bologna.

The initiative involved Haitian and Dominican institutions and consisted in two main components: (a) institutional capacity building on flood-risk management and mitigation measures and policies; (b) hydrological and hydraulic analysis of the May 2004 flood event aimed at formulating a suitable and affordable flood-risk mitigation plan. The second component of the cooperation is the main focus of this paper and in particular, starting from some logistical and technical constrains, a topographic survey based on GNSS technology that enabled us, in a short time, to survey river cross sections and construct Digital Elevation Models for two areas where to conduct numerical hydraulic modelling and to pre-design hypothetic flood-risk mitigation measures. The paper reports and discusses the main phases of the project.

From a technical point of view, different type of remote sensing considered, including terrestrial, satellite and aerial remote sensing. The choice is mainly based on the type of disaster and the approximate extent of the affected areas. Generally, the main source of data for response activities is satellite remote sensing, since it allows monitoring areas with accessibility issues with a wide footprint on the ground. Furthermore, modern agile satellites can be triggered in a very short time (first images showing the impact of the earthquake that struck Haiti were acquired the morning after the quake). As far as the temporal resolution is concerned, the recent availability of constellation drastically increase the satellite revisiting time, allowing to monitor in near real-time fast dynamic phenomena. Very high resolution (VHR) imagery (with a ground sample distance up to 0.5 m) are characterized by a very high level of detail that can be exploited not only from a geometric point of view (for map updating and creation purposes) but especially in terms of semantic content, crucial feature when assessing the impact of a disaster. On the contrary, high resolution imagery are characterized by a smaller footprint and a limited spectral resolution, characteristics that may limit the effectiveness of automatic classification algorithms as well as the use of this type of data when monitoring country-wide disasters.

Radar data are generally exploited when the persistency of cloud cover make optical data unusable or to extract very accurate information on ground displacements by means of phase data processing.

Particularly impressive seems to be the potentialities of UAV (Unmanned Aerial Vehicle) potentialities as described in Aicardi et al. In this paper the research group of Geomatics of the Politecnico di Torino has developed a set of interchangeable pods that can be mounted on a mini-UAV (a Hexacopter by Mikrokopter) devoted to emergency management in case of environmental disasters. This instrument is a low-cost mini-UAV equipped with photogrammetric sensors and capable of autonomous navigation (real time GNSS/IMU) and automatic digital image acquisition (characterized by a suitable geometric and radiometric quality). The platform is easily transportable on normal aircrafts and usable on the field, autonomously, by a couple of operators. The main innovation is to permits a real direct photogrammetric surveys in remote and disaster-affected areas in a short-range operative zone where it is not possible to carry out traditional photogrammetric flights. The acquisition technique allows the update of existing maps. Nevertheless, some test flights and practical applications have been performed in order to assess the autonomous flight performances and the suitability for photogrammetric flights.

As far as the damage assessment is concerned, up-to-date remotely sensed data are processed in order to extract the value added information required for that specific disaster type, i.e. flooded areas in case of flood events, collapsed buildings or temporary shelters in case of earthquakes, lava flows of ash fall contours in case of volcanic eruptions, ground displacements in case of mass movements, active fires or burned areas in case of forest fires. Depending on the type of input data available (optical or radar, panchromatic or multispectral, high or low spatial resolution, multi-temporal or just postevent acquisition) both semi automated and supervised classification algorithm, pixel based or object-oriented data can be exploited in order to derive the aforementioned information.

Unsupervised change detection algorithms are generally adopted when suitable pre event data are also available. Radar amplitude images can be processed in order to easily identify water bodies on the ground or to capture damaged areas by means of multi temporal SAR data processing, computing correlation coefficients or carrying out amplitude coherence analysis.

The availability of phase information allows adopting SAR interferometric analyses (InSAR) to provide information on the relative ground displacement after natural disasters.

It is important to stress the limits of remote sensing in assessing the impact of disasters, especially in urban environments, mainly due to intrinsic limits of vertical images. Georeferenced data acquired in the field are therefore crucial to correctly integrate and to validate the outcomes of the aforementioned analyses. Easy to- use GPS-based devices as well as crowdsourcing can be adopted to cope with the need of ground data and information.

The licensing policy of the data providers is another crucial feature that has to be carefully considered. International initiatives exist with the aim to supply remotely sensed data and/or related analyses when major disasters occur, such as the International Charter "Space and Major disasters," Sentinel Asia, Google Crisis Response and, in the framework of the European Programme Copernicus (formerly GMES - Global Monitoring for Environment and Security), GIO-EMS.

Remote sensing based analysis supports emergency management activities by providing the necessary georeferenced information to users in different formats and modalities. The response phase outputs are normally in shape of cartographic products where the value-added information (i.e. flooded areas) is integrated with cartographic reference datasets. As far as the warning phase is concerned, the common output is the approximate location of a disaster (i.e. earthquake epicenter, flood affected region), or, in case of alert based on forecasting models, the estimated location of the affected areas (i.e. coastal areas hit by a tsunami or a predicted storm path).

Dissemination process has the same importance as that of the analysis and map production phases. Final products should reach decision makers at the right moment and in the right place, taking into consideration environmental factors and potential network connectivity issues. Normal ways of dissemination includes email attachments sent to predefined mailing. Another dissemination option is the delivery to specific portals, focused on emergency management, that aim to gather the relevant and reliable information and analysis related to the latest emergencies (i.e. ReliefWeb). With the increasing dependence on geographical information, the demand for raw vector datasets that perform analysis better tailored to the end user needs is also increasing. Also, customized WebGIS applications are being largely implemented (and deployed immediately after specific disaster events) in order to distribute vector data that conform to OGC standards.

EVALUATION OF TRMM SATELLITE DATA FOR MAPPING MONTHLY PRECIPITATION IN PAKISTAN BY COMPARISON WITH LOCALLY AVAILABLE DATA

Muhammad Adnan Shahid[1,2,3], Piero Boccardo[2], Walther Cámaro García[1,2], Adriana Albanese[2] and Elena Cristofori[1,2]

[1]Ph.D student, Inter-University Department of Regional and Urban Studies and Planning, Politecnico di Torino, Italy
[2]ITHACA (Information Technology for Humanitarian Assistance, Cooperation and Action) Research Center, Politecnico di Torino, Italy
[3]Water Management Research Center, University of Agriculture, Faisalabad, Pakistan
E-mail of Corresponding Author 1: muhammad_shahid@polito.it

ABSTRACT

Increase in global average temperatures, widespread snowmelt and rising sea levels are important evidences of climate change, causing severe changes in the spatial and temporal rainfall patterns and increasing the frequency of related natural disasters like floods and droughts. This scenario increases the importance of satellite data for effective monitoring and forecasting of such disasters. Such data become more valuable in case of less developed countries where there is limited availability of local data. The open source and most commonly used data for detecting critical rainfall events are taken from Tropical Rainfall Measuring Mission (TRMM) Multi-satellite Precipitation Analysis (TMPA). This paper presents the evaluation of TRMM monthly rainfall data (3B43) for Pakistan, using 15 years data from 1998 to 2012 in comparison to the ground rainfall data for the same period. For calibration, regression analysis was performed for each month on the data of rain gauge stations and their corresponding pixel values from the satellite datasets. Regression equations were used to develop the calibrated seasonal and annual rainfall maps, as well as the monthly rainfall maps on district level. The calibrated monthly datasets were validated by calculating Nash-Sutcliffe Efficiency of TRMM estimates before and after calibration. The original TRMM 3B43 data was found quite reliable for its direct use with NSE values ranging from 0.73 to 0.92 for different months, while the calibration further improved the NSE by about 5% on average. However, the NSE values were decreased after calibration for the months of July, August and September, indicating that high accuracy and care is required along with much dense rain gauge network to perform calibration in hilly areas having local gradients and heavy orographic rainfalls during these rainy months. For dry months of winter, i.e. October to December, TRMM rainfall estimates were found relatively less accurate, but NSE values were improved by 10-15% after calibration in these months.

INTRODUCTION

Climate change impacts in terms of increased global temperatures and high spatio-temporal variability in rainfall patterns are being witnessed worldwide. These primary impacts are providing base for several inter-related issues and emerging challenges for water resources, agriculture, energy and other socioeconomic sectors. Increased frequency and severity of natural disasters like floods and droughts are also an important aspect of the adverse climate changes. Rainfall is an important factor of the hydrologic cycle and has key role in different phenomena like surface runoff generation and hydropower potential, occurrence of floods or droughts, and sustainable agriculture and food security. Therefore, the need for reliable and high resolution rainfall data, both spatial and temporal, is crucial for sound hydrologic studies and for timely detection and management of natural disasters like floods and droughts.

Rain gauges have been, and are still being considered a reliable source for providing reasonably accurate point rainfall measurements. However, point rainfall measurements do not provide true estimation of areal rainfall [1, 2], particularly when there exist local rainfall gradients as in case of Himalayas [3, 4, 5]. The areal rainfall estimation is mandatory at proper spatial and temporal scale for conducting studies at basin level [6].This scenario raises the importance of satellite data for effective monitoring of rainfall for conducting catchment level water studies and combating disasters. Use of such data becomes more important in case of developing countries where there is limited availability of local data in terms of sparse rain gauge network, which cannot detect rainfall variations caused by topography and orographic effects, and thus, results in erroneous estimates of areal rainfall [7].

Satellite-based precipitation products have become an important alternative source of information [8], under the need for more accurate spatially distributed rainfall estimates [9]. Some important remotely measuring precipitation instruments are active Precipitation Radar (PR), passive Microwave Radiometer (MWR) such as Tropical Rainfall Measuring Mission (TRMM) Microwave Imager (TMI) and Infrared Radiometer (IR)sensors [10, 11]. The active PR sensor records the three dimensional structure of the rainfall distribution [12]; IR observations provide indirect measurements at the top of clouds [10]; while the TMI detects the radiation emitted by the water fraction in the vertical profile of the atmosphere [13].

The TRMM Multi-satellite Precipitation Analysis (TMPA) provides very high temporal (3 hourly) and spatial (0.25^o x 0.25^o) resolution products using combination of sensing instruments. However, the indirect nature of precipitation measurement by the sensors shows some uncertainties too [14, 15], associated with lack of rainfall detection, false detection and bias [16]. Franchito et al. (2009) [17] have reported both temporal (8% to 12%) and sampling (30%) errors in satellite rainfall estimates.These biases and random errors may be due to sampling frequency, diurnal cycle of rainfall, non-uniform field of view of sensors, and the uncertainties in the rain retrieval algorithms [18, 19, 20, 21, 22, 23]. Therefore, satellite rainfall estimates are needed to be evaluated to reduce such errors, especially on regional basis instead of using global approximations [24, 25].

Many scientists have made efforts at global and regional scales for the evaluation of satellite products by comparing them with the field rainfall measurements, which showed varying accuracies in different regions and for different methods. Adeyewa and Nakamura (2003) [26] used Global Precipitation Climatology Center global-precipitation-analyses rain gauge data for comparison with TRMM Precipitation Radar (PR) data, the threshold-matched precipitation index and the TRMM-and-other-sources ‘‘best-estimate’’ data product (3B43) for 36 months over the major climatic regions in Africa. They found close agreement of 3B43 product with the rain gauge data, and even used it as a substitute of rain gauge data over the South Atlantic Ocean for the validation of other satellite products. Ji and Stocker (2003) [27], and Chokngamwong et al. (2005) [28] observed correlations of 0.56 and 0.86 between the satellite and rain gauge measurements, respectively. Dinku et al. (2007) [29] estimated Nash–Sutcliffe efficiency of 0.81 and root mean square error of 25%between the satellite and rain gauge data averaged over 2.5^o grid boxes. The accuracy for a single 25 km×25 km pixel containing 23 rain gauges in Oklahoma was tested by Villarini and Krajewski (2007) [30] and a correlation of 0.55 was found between the satellite and rain gauges values. Cheema and Bastiaanssen (2012) [31] performed calibration of TRMM 3B43 data product for the year of 2007 over Indus basin using regression analysis and geographical differential analysis techniques. They reported decrease from pre-calibration to post-calibration deviation between TRMM data and rain gauge data to be 10.9% to 6.1% for annual time periods, and 34.9% to 15.4% for monthly periods.

This paper presents the evaluation of TRMM monthly data (3B43) over 15 years from 1998 to 2012 for Pakistan to investigate its scope for detection and management of natural disasters like droughts and floods. Monthly rainfall products at high spatial resolution are very useful for conducting drought studies, but daily or even 3-hourly datasets (TRMM 3B42) are considered better to conduct sound rainfall-runoff studies and managing floods. However, it is worth mentioning that the TRMM research datasets also incorporate the monthly rain gauge data for automated calibration [9]. For this purpose, the available 3-hourly estimates are summed over the calendar month to create a monthly multi-satellite (MS) product, which is then combined to monthly gauge data using inverse-error variance weighting, as reported by Huffman (1997) [24, 32], to create a post-real-time monthly satellite-gauge combination (SG) product, known as TRMM 3B43 product. Then for each grid box, monthly SG/MS or 3B43/MS ratio is computed and applied to each 3-hourly field in the month, producing the final 3B42 product. Thus, it is believed that the evaluation of monthly product (3B43) for an area might also help in providing guidelines for the use of daily and hourly products.

MATERIALS AND METHODS

Description of Study Area

Pakistan is one of the developing countries, covering an area of 79.6 Mha and represents a region which is highly prone to climate change. Ranging from coastal areas along the Arabian Sea in south to the glaciated mountains in north (Figure 1), Pakistan possesses a landscape having high diversity in terms of plains, deserts, plateaus, hills and glaciers. Geographically and from water resources point of view, Pakistan can be divided into three major parts: the northern highlands and north-eastern Himalayan mountains contributing by snowmelt and rainfall to the mighty Indus Riverand its tributaries; the Indus River plain which covers major area of Pakistan including KP, Punjab and Sind provinces; and the Balochistan province which lies in the south-west and is mostly under drought conditions due to arid climate. Major part of Pakistan is under arid to semi-arid climate with relatively higher rainfalls in the northern areas and lower towards the middle and south. Two important sources of rainfall are monsoon causing heavy rainfalls and frequent flooding from June to September, and the western disturbances contributing in terms of rain and snowfall over hilly areas during winter. However, there is high variability in seasonal rainfalls with monsoon season contributing alone to about 70% of annual rainfall, and dry months of October and November with almost no rain. In addition to seasonal differences, annual rainfall also varies greatly from year to year and occurrences of alternate flooding and drought are common.

Data Availability

The satellite rainfall data used in this study were obtained from TRMM Multi-satellite Precipitation Analysis (TMPA), which makes use of the microwave and infrared precipitation estimates by the TRMM's onboard instruments as well as integration of the monthly rain gauge data for the post-real-time research products. The instruments onboard TRMM include Precipitation Radar (PR), Microwave Imager (TMI), Visible and Infrared Scanner (VIRS), Clouds and the Earth's Radiant Energy System (CERES), and the Lightning Imaging Sensor (LIS). Different types of TRMM products are available on NASA's website; monthly rainfall product (TRMM 3B43) was downloaded and processed for 15 years from 1998 to 2012 using ftp protocol and Python code for automated conversion of data into Geo-TIFF format for their use in ArcMap.

For calibration purposes monthly ground rainfall data over the same period of 15 years for 35 rain gauge stations were obtained from Pakistan Meteorological Department (PMD); the location of stations is shown in Figure 1. Although the rain gauge network is sparse compared to the vastness of area [31], this was the only reliable source of ground rainfall data. Rain gauges may also have some errors, but are normally considered correct and true representative of point rainfall [31, 33] in a basin for validation of other datasets. Moreover, use of 15 years data to have average annual and monthly rainfall values, both for satellite and rain gauge data, may be considered helpful in neutralizing any biases in both datasets.

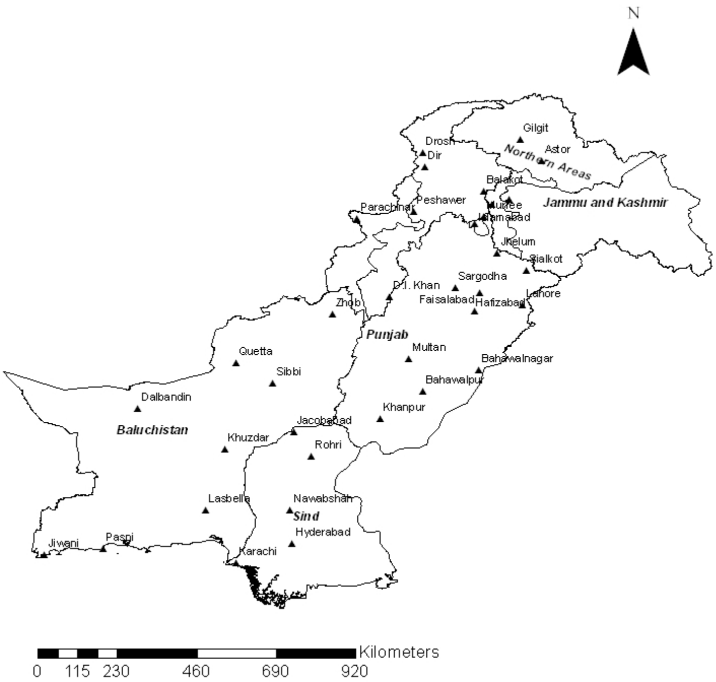

Fig. 1 - Map of Pakistan with provincial boundaries and location of rain gauge stations used in this study.

Calibration using Regression Analysis

There have been found a relationship between the TRMM rainfall estimates and rain gauge observations by many scientists [26, 8, 31]. The empirical relations were developed for each month using regression analysis on data from 29 rain gauge stations and the corresponding pixels in TRMM grid data which were identified using spatial join overlay technique in ArcMap. Data for remaining six rain gauge stations were used for validation purposes only, following the calibration and validation stations ratio adopted by Cheema and Bastiaanssen (2012) [31]. To have best relationships and address the non-linearity in both datasets, second order polynomial equations were developed with zero intercept, which can be described as:

$$R_{cal} = R_{gauge} = a\,(R_{TRMM})^2 + b\,(R_{TRMM}) \qquad (1)$$

WhereR_{cal} is the resulting calibrated TRMM rainfall, R_{TRMM} is the TRMM rainfall from original 3B43 product, and 'a' and 'b' are the regression coefficients for the calibration of 3B43 product for Pakistan.

Development of Calibrated Rainfall Maps

By the use of developed calibration equations for each month, new monthly rainfall raster, and in turn, the seasonal (six monthly) and annual raster datasets were developed using map algebra tool. The year was divided into two six monthly parts keeping in view the two prevailing cropping seasons in Pakistan, i.e. Rabi (from November to April) representing the relatively dry winter and a bit hot spring with rainfall currents due to western disturbances, and Kharif (from May to October) representing the hot summer and rainy season having heavy monsoon rains, but also a part of the post- monsoon season in October with almost no or very less precipitation. To have district level monthly satellite rainfall maps for Pakistan, the calibrated raster datasets were converted to polygon or vector files which were combined with the vector file of local administrative/district boundaries. Union of the two layers with defining proper statistical parameters resulted in estimating average monthly rainfall for each administrative division.

Validation

For performance evaluation and validation of the original TRMM data and the calibrated rainfall maps, six remaining rain gauges' measurements and their respective pixel values were used to estimate Nash-Sutcliffe Efficiency (NSE) for each month. NSE determines the relative magnitude of noise in estimated data compared to the measured data [34], using following relation:

$$NSE = 1 - \frac{\sum_{i=1}^{n}(R_{rgs} - R_{trmm})^2}{\sum_{i=1}^{n}(R_{rgs} - \langle R_{rgs} \rangle)^2} \quad (2)$$

Where R_{rgs} is the measured/observed rainfall for a specific rain gauge, R_{trmm} is the satellite rainfall value for the respective pixel, $\langle R_{rgs} \rangle$ is the mean observed rainfall, and n is the total number of observations or rain gauge stations used for the validation purpose. Value of NSE ranges from -∞ to 1; values between 0.0 and 1.0 are generally considered as acceptable, while the values less than 0.0 indicate that the observed mean is more accurate than the estimated value, which is unacceptable. NSE was calculated for each month as well as for the whole year to evaluate the accuracy of TRMM 3B43 product and the performance of calibration work using the pre-calibration and post-calibration satellite rainfall maps, respectively.

RESULTS AND DISCUSSION

Figure 2 shows the comparison of satellite rainfall with rain gauge measurements for all the months, along with the resulting second order polynomial equations and respective R^2 values.

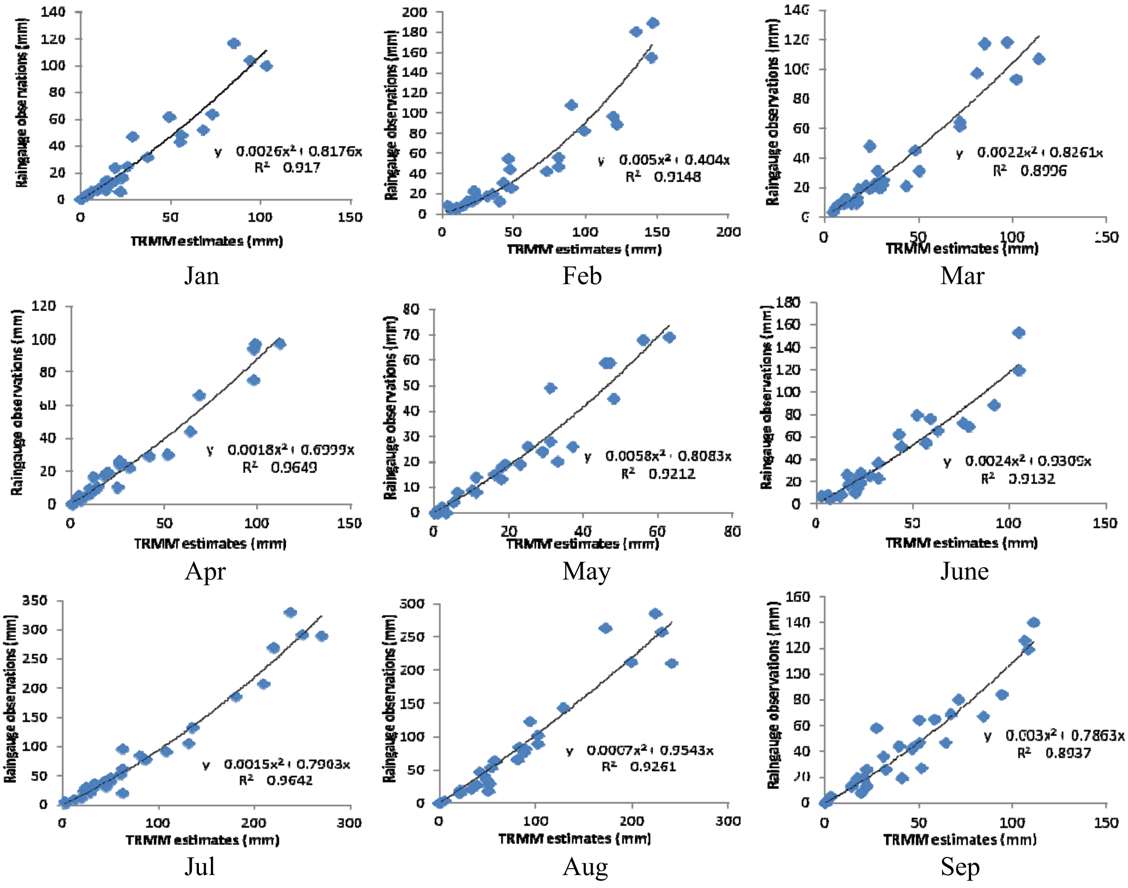

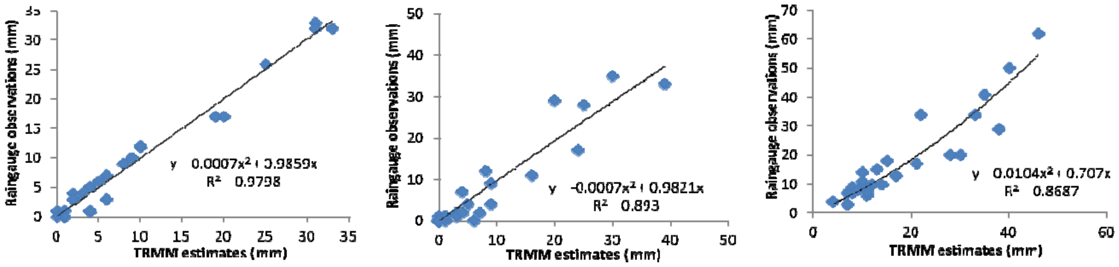

Oct Nov Dec

Fig. 2 - Regression analysis for 15 years' mean precipitation values of 29 rain gauges vs TRMM 3B43.

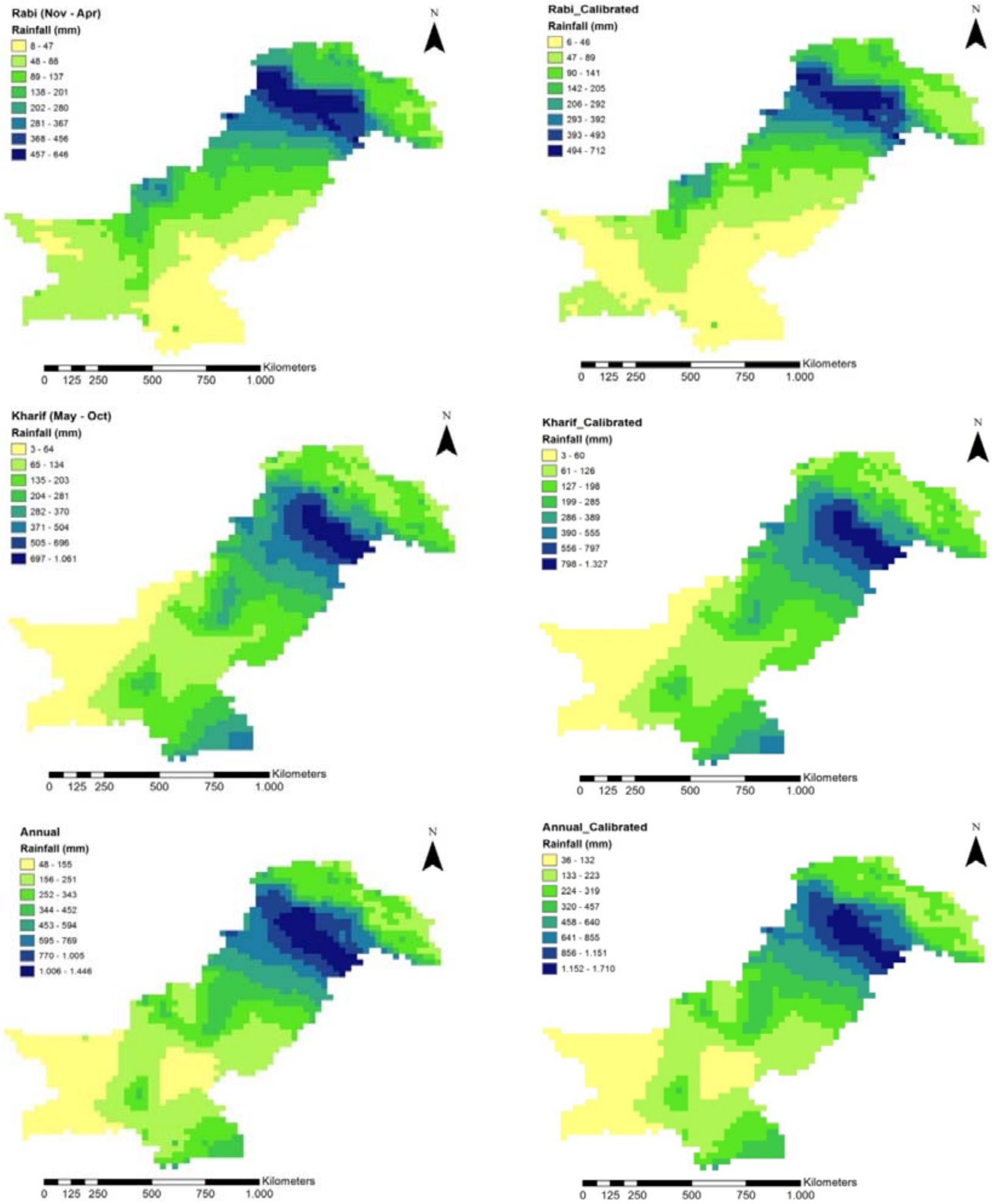

Fig. 3 - Seasonal and annual maps of satellite rainfall before and after calibration.

For most of the months, resulting curves were of the parabolic form with their convection towards horizontal axis, indicating that the overall TRMM satellite estimates are on higher side a little, but leading to the underestimation at higher rainfall values; similar trends were experienced by other scientists [28, 35, 31]. However, almost linear behavior was seen for the months of October and November, as the total rainfall in these months was very low, i.e. up to 40 mm month^{-1}. Therefore, it can be seen that actually these lines represented just the lower one-third part approximately of the curves for other months, and thus, showed almost a linear behavior with little overestimation by the satellite. High correlation was found between two datasets for all months with R^2 values ranging from 0.87 for December to 0.98 for October.

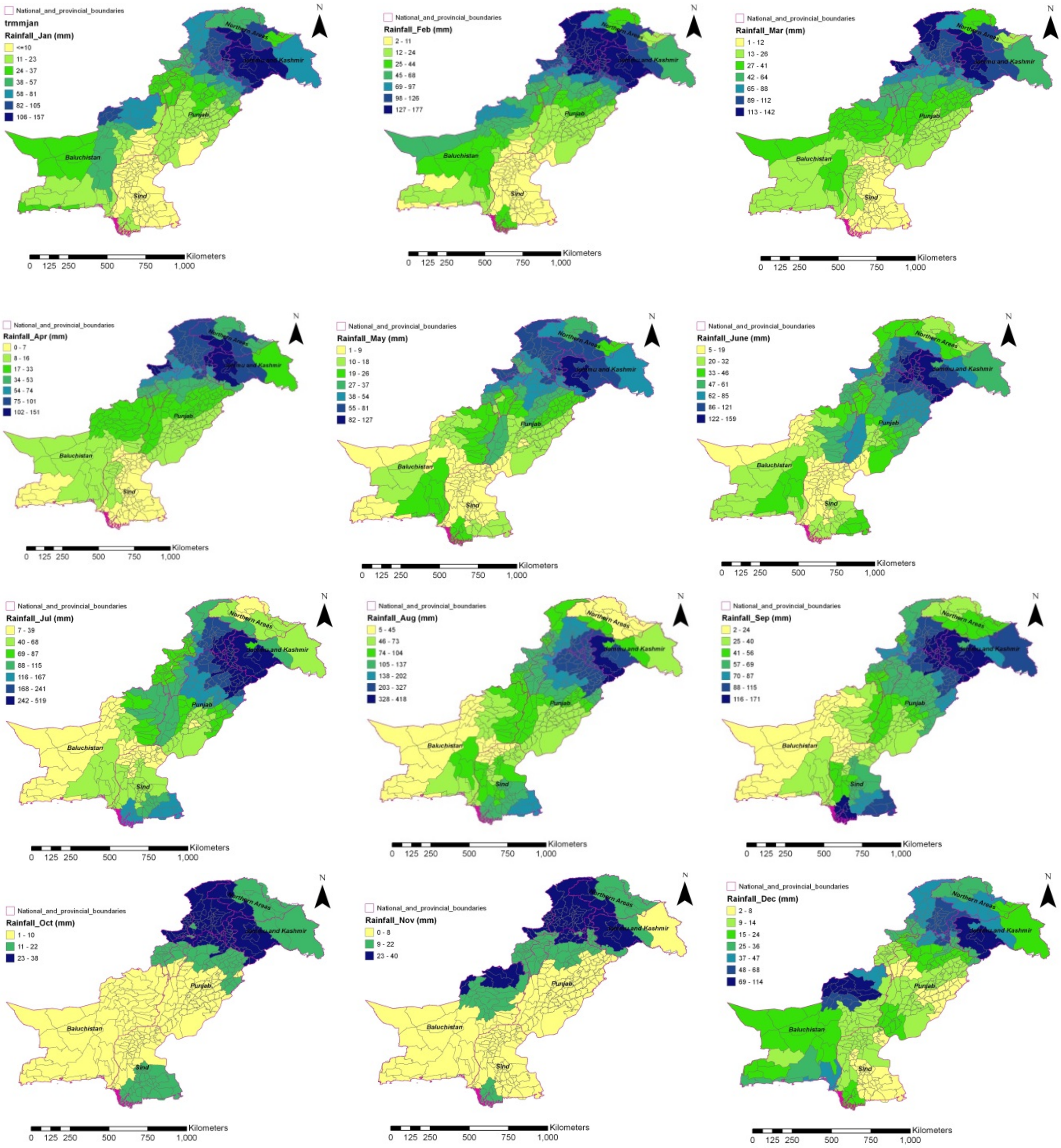

Fig. 4 - District level monthly satellite rainfall maps.

The seasonal and annual raster maps before and after the calibration of satellite data have been shown in Figure 3. From Figure 3, it can be seen that in Rabi season, representing the low rainfall winter and spring season, calibration work improved the satellite data and there was found a shift of south-western areas (Balochistan province) from rainfall class of 45-90 mm to that of below 45 mm. Similar little variations were found in the distribution of other classes before and after calibration. For Kharif season, representing the summer and monsoon rainfall season, the distribution of rainfall classes was found almost similar before and after calibration; and similar was the case for the whole year mapping. The upper Punjab province areas, which are at the foot hills of Himalayan Mountains, were found under heavy rainfall in Kharif season due to monsoon winds and orographic effects. The annual maps show that the upper Punjab foot hills areas and upper KP province are under severe climate change impacts in terms of heavy rainfall, which mostly result in flooding in the downstream areas of KP, Punjab and Sind provinces. South-western areas in Balochistan province and some desert areas in the north-eastern Sind province were found under the severe drought risks with arid climate having average annual rainfall in the range of 35-135 mm. Areas in the southern Punjab and the belt along the mutual boundary of Sind and Balochistan provinces were also found under arid to semi-arid climate with average annual rainfall in the range of 135-225 mm, thus having threat for agriculture in terms of temporary crop water stresses. For further understanding of spatio-temporal rainfall variations, monthly rainfall maps on district level were also developed (Figure 4), which can be highly helpful for having idea of monthly average rainfall for each district and planning strategies for pre-event management of flooding and/or water shortage periods.

For validation purposes, monthly and annual values of Nash-Sutcliffe Efficiency (NSE) for pre and post calibration TRMM rainfall estimates are presented in Table 1, and their variations within the year from month to month are further elaborated in Figure 5. Table 1 show that TRMM rainfall estimates even without calibration were found as a useful source of rainfall grid data in comparison to sparse rain gauge network, having NSE values in the range of 0.73 to 0.92. The calibration work performed in this study further improved the NSE values for the satellite rainfall estimates, but this improvement was only about 5% on the average. It is important to mention that the NSE values were found high (0.85-0.95) in the summer and monsoon months, i.e. from April to September due to relatively heavy rainfalls during these months, but the calibration approach even decreased the NSE values for the rainy months of July, August and September. Reasons for this extraordinary result were investigated and major deviations between rain gauge and pixel values causing low NSE values during these months were found for the hilly rain gauge stations, which are under high wind and orographic effects during the monsoon period. In these areas during monsoon season, there may be high variations in rainfall from pixel to pixel and even within a pixel covering an area of about 25 x 25 km^2, thus any comparison or calibration in these areas using sparse rain gauge network may further increase the biases [31]. Table 1 and Figure 5 show that the lowest NSE values were recorded for the months of October, November and December; but the accuracy was greatly improved here by the calibration work resulting in an increase of 10-15% in the NSE values. This finding also matches with the results of other scientists [5, 31], who stated that TRMM overestimates the low rainfall, but very low rainfall rates are difficult to measure by the precipitation radar (PR) of TRMM due to detection limitation. Thus the accuracy of satellite rainfall estimates was found a little lower in these months, but greatly improved by the calibration work because high wind speeds and orographic effects were almost absent in these months.

Tab. 1 - Pre and post calibration NSE values for TRMM rainfall estimates

Month	Pre-calibrated NSE	Post-calibrated NSE
January	0.81	0.83
February	0.85	0.89
March	0.81	0.83
April	0.89	0.91
May	0.92	0.94
June	0.92	0.95
July	0.92	0.89
August	0.91	0.89
September	0.84	0.81
October	0.75	0.84
November	0.77	0.85
December	0.73	0.83
Overall Value	0.89	0.91

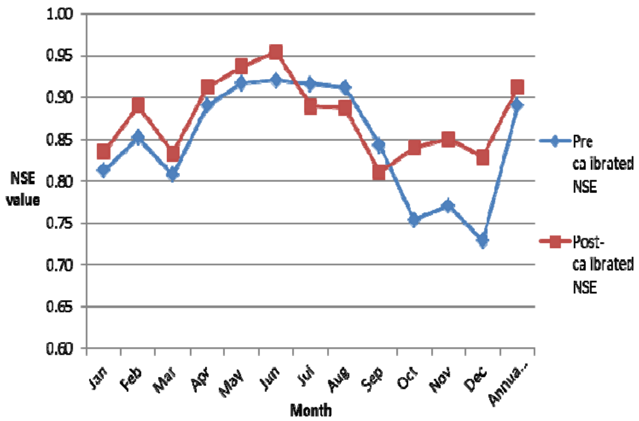

Fig. 5 - Variations in pre and post calibration NSE values from month to month.

SUMMARY AND CONCLUSIONS

TRMM rainfall products have become an important source of high spatio-temporal resolution grid data for their use in climate change and water resources studies. Many scientists have conducted studies for the evaluation of TRMM data in different parts of the world, as well as in Indus Basin covering the major area of Pakistan. This study was novel in this sense that 15 years data from the initiation of TRMM program, i.e. 1998 to 2012 was utilized, with the assumption that averaging of both the satellite and rain-gauge datasets over the period of 15 years will help neutralizing the errors and biases in both datasets. The study concluded that TRMM data are quite reliable for their direct and real time use for conducting any rainfall-based studies. For conducting high accuracy studies, these can be further calibrated by adopting suitable calibration techniques. However, for high mountainous areas with heavy orographic rainfalls, regional calibration should be performed very carefully and for limited areal extents using as much dense and uniformly distributed rain gauge network as possible.

ACKNOWLEDGEMENTS

This study was technically supported by ITHACA Research Center regarding TRMM satellite data processing and use. The authors also acknowledge Pakistan Meteorological Department (PMD) for providing rain gauge stations data. Special thanks to Higher Education Commission (HEC), Pakistan for providing financial support in the form of PhD scholarship to conduct research activities.

REFERENCES

[1] Draper, C.S., J.P. Walker, P.J. Steinle, R.A.M. Dejeu and T.R.H. Holmes, "An evaluation of AMSR-E derived soil moisture over Australia," Remote Sensing of Environment, vol. 113, pp. 703 - 710, 2009.
[2] Tustison, B., D. Harris and E. Foufoula-Georgiou, "Scale issues in verification of precipitation forecasts", J. Geophys. Res., vol. 106, no. D11, pp. 11775 - 11784, 2001.
[3] Barros, A.P., G. Kim, E. Williams, and S.W. Nesbitt, "Probing orographic controls in the Himalayas during the monsoon using satellite imagery", Nat. Hazards Earth Syst. Sci., vol. 4, no. 1, pp. 29 - 51, 2004.
[4] Bhatt, B.C., and K. Nakamura, "Characteristics of monsoon rainfall around the Himalayas revealed by TRMM precipitation radar", Mon. Weather Rev., vol. 133, no. 1, pp. 149 - 165 , 2005.
[5] Anders, A.M., G.H. Roe, B. Hallet, D.R. Montgomery, N.J. Finnegan, and J. Putkonen, "Spatial patterns of precipitation and topography in the Himalaya", GSA Spec. Pap., vol. 398, pp. 39 - 53, 2006.
[6] Sawunyama, T. and D.A. Hughes, "Application of satellite-derived rainfall estimates to extend water resource simulation modelling in South Africa", Pretoria: Water Research Commission, vol. 34, pp. 1 - 9, 2008.
[7] Andréassian, V., C. Perrin, C. Michel, I. Usart-Sanchez, and J. Lavabre, "Impact of imperfect rainfall knowledge on the efficiency and the parameters of watershed models", Journal of Hydrology, vol. 250, pp. 206 - 223, 2001.
[8] Din, S.U., A.A. Dousari, A. Ramdan, and A.A. Ghadban, "Site-specific precipitation estimate from TRMM data using bilinear weighted interpolation technique: an example from Kuwait", Journal of Arid Environments, vol. 72, pp. 1320-1328, 2008.
[9] Huffman, G.J., R.F. Alder, M.M. Morrissey, D.T. Bolvin, S. Curtis, R. Joyce, B. Mcgavock, and J. Susskind, "Global precipitation at one-degree daily resolution from multisatellite observations", Journal of Hydrometeor., vol. 2, pp. 36-50, 2001.
[10] Huffman, G.J., R.F. Adler, D.T. Bolvin, G. Gu, E.J. Nelkin, K.P. Bowman, Y. Hong, E.F. Stocker, and D.B. Wolff, "The TRMM Multisatellite Precipitation Analysis (TMPA): Quasi-global, multiyear, combined-sensor precipitation estimates at fine scales", Journal of Hydrometeorology, vol. 8, no. 1, pp. 38-55, 2007.
[11] Ushio, T., K. Sasashige, T. Kubota, S. Shige, K. Okamoto, K. Aonashi, T. Inoue, N. Takahashi, and T. Iguchi, "A Kalman filter approach to the Global Satellite Mapping of Precipitation (GSMaP) from combined passive microwave and infrared radiometric data", J. Meteorol. Soc. Jpn., vol. 87A, no. 9, pp. 3084-3097, 2009.
[12] Kummerow, C., W. Barnes, T. Kozu, J. Shiue, and J. Simpson, "The Tropical Rainfall Measuring Mission (TRMM) sensor package", J. Atmos. Oceanic Technol., vol. 15, no. 3, pp. 809-817, 1998.
[13] Kubota, T., S. Shige, H. Hashizume, K. Aonashi, N. Takahashi, S. Seto, Y.N. Takayabu, T. Ushio, K. Nakagawa, K. Iwanami, M. Kachi, and K. Okamoto, "Global precipitation map using satellite-borne microwave radiometers by the GSMap project: Production and validation", Geoscience and Remote Sensing, vol. 45, no. 7, pp. 2259-2275, 2007.
[14] Hong, Y., K.L. Hsu, H. Moradkhani, and S. Sorooshian, "Uncertainty quantification of satellite precipitation estimation and Monte Carlo assessment of the error propagation into hydrologic response", Water Resources Research, vol. 42, 2006.
[15] Hossain, F., E.N. Anagnostoub, and A.C. Bagtzoglou, "On Latin hypercube sampling for efficient uncertainty estimation of satellite rainfall observations in flood prediction", Computers and Geosciences, vol. 32, pp. 776-792, 2006.
[16] Tobin, K.J., and M.E. Bennett, "Adjusting satellite precipitation data to facilitate hydrologic modelling", Journal of Hydrometeorology, vol. 11, pp. 966-978, 2010.
[17] Franchito, S.H., V.B. Rao, A.C. Vasques, C.M.E. Santo, and J.C. Conforte, "Validation of TRMM precipitation radar monthly rainfall estimates over Brazil", Journal of Geophysical Research, vol. 114, 2009.
[18] V.E. Kousky, "Diurnal rainfall variation in northeast Brazil," Mon. Wea. Rev., vol. 108, pp. 488-498, 1980.
[19] Bell, T.L., A. Abdullah, R.L. Martin, and G.R. North, "Sampling errors for satellite-derived tropical rainfall: Monte Carlo study using a space-time stochastic model", Journal of Geophysical Research, vol. 95, pp. 2195-2206, 1990.
[20] Chiu, L.S., D. Short, A. McConnel, and G. North, "Rain estimation from satellites: Effect of finite field of view", Journal of Geophysical Research, vol. 95, pp. 2177-2185, 1990.
[21] C. Kummerow, "Beamfilling errors in passive microwave rainfall retrievals", J. Appl. Meteor., vol. 37, pp. 356-357, 1998.
[22] Anagnostou, E.N., W.F. Krajewski, and J.A. Smith, "Uncertainty quantification of mean-areal radar-rainfall estimates", Journal of Atmos. Oceanic Technol., vol. 16, pp. 206-215, 1999.

[23] Chang, A.T.C., and L.S. Chiu, "Nonsystematic errors of monthly oceanic rainfall derived from SSM/I," Mon. Wea. Rev., vol. 127, pp. 1630-1638, 1999.
[24] G.J. Huffman, "Estimates of root-mean-square random error for finite samples of estimated precipitation", J. Appl. Meteor., vol. 36, pp. 1191-1201, 1997.
[25] Kummerow, C., and Coauthors, "The status of the Tropical Rainfall Measuring Mission (TRMM) after two years in orbit," J. Appl. Meteor., vol. 39, pp. 1965-1982, 2000.
[26] Adeyewa, Z.D., and K. Nakamura, "Validation of TRMM radar rainfall data over major climatic regions in Africa", Journal of Appl. Meteor., vol. 42, pp. 331-347, 2003.
[27] Ji, Y., and E. Stocker, "Ground validation of TRMM and AMSU microwave precipitation estimates", in Proceedings of the International Geoscience and Remote Sensing Symposium, Toulouse, France, 2003, pp. 3157-3159, July 21-25.
[28] Chokngamwong, R., L. Chiu, and J. Vongsaard, "Comparison of TRMM rainfall and daily gauge data in Thailand", in Spring Meeting 2005 of American Geophysical Union, 2005.
[29] Dinku, T., P. Ceccato, E. Grover-Kopec, M. Lemma, S.J. Connor, and C.F. Popelewski, "Validation of satellite rainfall products over East Africa's complex topography," International Journal of Remote Sensing, vol. 28, pp. 1503-1526, 2007.
[30] Villarini, G., and W.F. Krajewski, "Evaluation of the research version TMPA three-hourly 0.25 x 0.25 rainfall estimates over Oklahoma", Geophysical Research Letters, vol. 34, 2007.
[31] Cheema, M.J.M., and W.G.M. Bastiaanssen, "Local calibration of remotely sensed rainfall from the TRMM satellite for different periods and spatial scales in the Indus Basin", Int. J. of Remote Sensing, vol. 33, no. 8, pp. 2603-2627, 2012.
[32] R. Vigna, "Early warning systems for risk management: design and implementation of a global early warning system for heavy rainfall detection", Department of Land, Environment and Geo-engineering, Politecnico di Torino, PhD Thesis 2011.
[33] Vila, D.A., L.G.G. De Goncalves, D.L. Toll, and J.R. Rozante, "Statistical evaluation of combined daily gauge observations and rainfall satelite estimates over Continental South America," Journal of Hydrometerology, vol. 10, pp. 533-543, 2009.
[34] Nash, J.E., and J.V. Sutcliffe, "River flow forecasting through conceptual models part 1 - a discussion of principles", Journal of Hydrology, vol. 10, pp. 282-290, 1970.
[35] Islam, N.M., and H. Uyeda, "Vertical variations of rain intensity in different rainy periods in and around Bangladesh derived from TRMM observations", International Journal of Climatology, vol. 28, pp. 273-279, 2008.

FLOOD-RISK MITIGATION IN THE SOLIETTE RIVER BASIN: AN INTERNATIONAL COOPERATION INITIATIVE (HAITI, DOMINICAN REP., ITALY)

A. Domeneghetti[*], S. Gandolfi[*], M. Barbarella[*], A. Castellarin[*], L. Brandimarte[°], G. Di Baldassarre[°], A. Brath[*]

[*]DICAM University of Bologna, Italy, alessio.domeneghetti@unibo.it
[°]UNESCO-IHE Institute for Water Education, Delft, The Netherlands, l.brandimarte@unesco-ihe.org

ABSTRACT

Isla Hispaniola (Haiti and the Dominican Republic), one of the poorest regions of the planet, has repeatedly been hit by catastrophic natural disasters that caused incalculable economic losses and killed thousands of people. One striking example is the disastrous flood-event that occurred in the transnational basin of River Soliette on May 24th, 2004. The event was produced by a severe tropical storm originated over the Caribbean Sea from an intense low-pressure system, and killed over 1000 Haitian and Dominican people, wiping out a number of rural villages. The General Direction for Development and Cooperation of the Italian Department of Foreign Affairs funded through the Istituto Italo-Latino Americano (IILA, www.iila.org) an international cooperation initiative (ICI), coordinated and directed by the University of Bologna. The initiative involved Haitian and Dominican institutions and consisted in two main components: (a) institutional capacity building on flood-risk management and mitigation measures and policies; (b) hydrological and hydraulic analysis of the May 2004 flood event aimed at formulating a suitable and affordable flood-risk mitigation plan. The second component of the cooperation is the main focus of this paper and in particular, starting from some logistical and technical constrains, a topographic survey based on GNSS technology that enabled us, in a short time, to survey river cross sections and construct Digital Elevation Models for two areas where to conduct numerical hydraulic modelling and to pre-design hypothetic flood-risk mitigation measures. The paper reports and discusses the main phases of the project.

KEY WORDS: *FLOOD RISK MITIGATION PLAN, TRANS-BOUNDARY CATCHMENT, GNSS, DEM*

INTRODUCTION

Over the last decades the island shared by Haiti and the Dominican Republic, known as Isla Hispaniola (see Figure 1), has been affected by a number of severe hydrological events that causes thousand fatalities and incalculable damages to structures and environment. One of the most devastating and striking example is represented by the catastrophic flood occurred on May 24th, 2004, where a tropical depression in the Caribbean Sea caused a flash-flooding in the transnational basin of River Soliette, causing floods and landslides. According to the estimation provided by the US Angency for International Development [1], the event hit the larger urban settlements of the catchment, destroying a large part of Jimanì (on the Dominican part of the catchment; see Figure 1) and Fond Verrettes (on the Haitian side of the river basin; see Figure 1), killing over 1000 Haitian people and more than 400 people in the Dominican Republic wiping away several rural villages.

The extremely high hydro-geological risk of the Isla Hispaniola seems to be the result of a combination of different factors, such as the meteorological exposition of the area (i.e. the high frequency with which the island is hit by extreme events) and the high vulnerability of the territory. In particular, this latter aspect has been significantly accentuated by an uncontrolled development of human activities (e.g. the intense process of deforestation) and unplanned urban expansions which interest the whole river catchment.

In this context, developed countries should assist emerging countries in the field of flood-risk mitigation and flood protection planning, providing local technicians with the required instruments and knowledge necessary for the identification and implementation of structural and non-structural measures aimed at the reduction of the hydraulic risk.

It was in this perspective that the General Direction for Development and Cooperation of the Italian Department of Foreign Affairs funded through the Istituto Italo-Latino Americano (IILA, www.iila.org) an international cooperation initiative (ICI), coordinated and directed by the University of Bologna (UniBo). The ICI involved local experts, public bodies and institutions (i.e., Secretaria de Estado de Medio Ambiente, SEMAR, and Instituto Nacional de Recursos Hidráulicos, INDRHI - http://www.indrhi.gob.do - in Dominican Republic, Ministère de l'Agricolture, des Ressources Naturelles et du Développment Rural, MARNDR - http://www.agriculture.gouv.ht - in Haiti), pursuing three main objectives: *(a)* institutional capacity building in the context of flood-hazard assessment and flood-risk management for Haitian and Dominican experts working on local public institutions; *(b)* investigation of the hydrological and hydraulic behaviour of the River Soliette (i.e. reconstruction and numerical simulation of the May 2004 event); *(c)* relative to the prototypical case study of Soliette trans-boundary river-basin, identification of guidelines for the development of flood-risk mitigation plans and for the selection and pre-design of the most suitable structural ad non-structural mitigation and adaptation measures.

Referring to this experience the paper summarizes the ensemble of activities implemented in the different context of the ICI. In particular, it reports a general overview for what concern the institutional capacity building and the hydrological reconstruction of the May 2004 event (objectives *(a)* and *(b);* deeply investigated and described by Brandimarte et al. [2]), while it mainly focuses on the topographical and hydraulic analysis carried out for the evaluation of flood-risk mitigation measures for the upper part of the catchment (objective *(c)*). In relation to the latter point, even if the manuscript does not present new instruments or methodological applications it reports a valuable way to reconcile topographic and geometric data required for the application of hydraulic numerical models with the necessity to operate in remote areas, where unfavourable operational (i.e. limited economic resources) and environmental conditions are combined together, avoiding the possibility to use up-to-date instrumentation and survey procedures (i.e. LiDAR or photogrammetric survey).

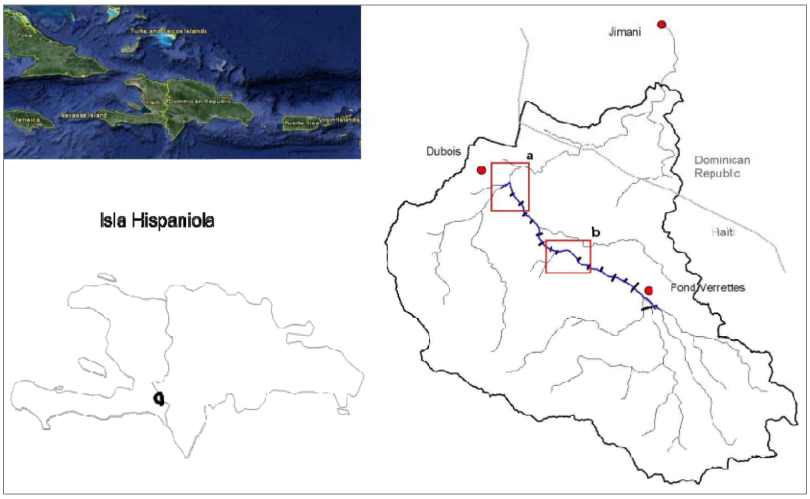

Fig. 1 - Trans-boundary catchment of the River Soliette: principal hydrograph network (black tin line), modeled reach (blue tick line) and river cross-sections (black segments); red boxes identify the areas of interest for detailed topographic surveys.

INSTITUTIONAL CAPACITY BUILDING

The institutional capacity building involved 12 junior local engineers (6 from Dominican Republican and 6 from Haiti) working for local public bodies or institutions (i.e. INDRHI, SEMAR and MARNDR) who attended a series of master classes for an overall period of 9 months. These classes, organized and coordinated by a pool of Italian researchers of the UniBo, focused on the fields of integrated water resources management and flood-risk mitigation, deepening in particular the following issues: hydrology and fluvial hydraulics analysis, hydrologic statistics, geographical information systems (GISs), topographical and geological analysis of the Isla Hispaniola, water distribution systems, structural and non-structural measures for flood-risk mitigation.

Since the final aim of the initiative was to enable 12 junior engineers to elaborate a possible flood-mitigation plan for the trans-boundary catchment, the master classes were also supported by practical activities through several computational experiments and field trips (see Figure 2).

These field trips were not only useful for participants' awareness about the damages of the May 2004 flood event, but they also provided the opportunity to better understand people habits, water education and awareness about the flood risk associated to the river Soliette. Furthermore, some of those field activities also focussed on the implementation of a detailed topographical survey of the upper part of the basin, providing a valid example on how to reconcile topographic data requirements for numerical hydraulic models in the context of flood-risk assessment in remote areas.

HYDROLOGICAL ANALYSIS AND FLOOD-RISK MITIGATION PLAN

Study area and numerical reconstruction of the May 2004 event

The study area is represented by the trans-boundary catchment of River Soliette (Figure 1), situated in the southern part of the Isla Hispaniola. The overall extension of the drainage area is c.a. 135 km^2, of which about 20% (lower basin) belongs to the Dominican Republic, while the remaining part (upper basin) belongs to Haiti. Stream-channel slopes range from 17% (upper basin) to 2% (lower basin) and it is often characterized by zero-flow period during most years. The two main urbanized areas in the basin are Fond Verrettes, in Haiti, and Jimaní, in the Dominican Republic (red dots in the Figure 1). Fond Verrettes lies on a wide plain area in the Haitian mountain side of the River Soliette, surrounded by steep slopes. During years preceding the 2004 flood event Fond Verrettes and Jimaní extended, getting in proximity to the main channel (Fond Verrettes), or occupying rather large portions of the alluvial bed of the River Soliette (Jimaní). Evidently, the unplanned and uncontrolled expansion of Fond Verrettes and Jimaní increased significantly the vulnerability of the area to flooding.

Fig. 2 - Institutional capacity building through theoretical and field trips activities (left and central panels) and a statement of Environmental Educational activities for the population living in the flood prone area (right panel).

In addition, since the extreme poverty conditions of this particular area, the wood represents the main source of energy for the population of the island, with the result that the Haitian territory is affected by an intense deforestation process along the steep slopes of the river basin (see Figure 3). Especially in the upper and central part of the catchment (Figure 1), due to steep slopes (around 17% on the upper basin) and deforestation process that increase the soil erodibility, flash-floods can move large volumes of sediments and represent a big risk for urban areas situated along the reach or in the lower part of the catchment (i.e. Jimaní). As a consequence of this condition, the May 2004 event, characterized by extreme rainfall intensity, was also characterized by an intensive sediment transport, in some cases with boulder of about 2-3 m that were responsible for most of the damages (Figure 3).

Fig. 3 - Pictures taken from the basin of the River Soliette: example of the extensive deforestation process in the upper part of the basin (pictures on the left side) and pictures taken after the May 2004 event highlighting the erosion process and the dimension of transported boulders (pictures on the right side).

Concerning the study area, since the absence of a systematic measurement network in the river basin, the available hydraulic information was very sparse and referred only to low-flow conditions [3]. In this conditions in which historical information on flood events are particularly limited it is not possible to implement a traditional flood frequency analysis for the estimation of hydrological events associated with a specific return period. Starting from these considerations, in order to evaluate the hydraulic behavior of the River Soliette during severe hydraulic conditions, the study refers to the May 2004 event. Even if two previous studies provided an estimation of the peak flow at Jimanì [4][5], Brandimarte et al. [2] provided a first comprehensive hydrological analysis of the May 2004 event. Taking advantage of the collaboration between Haitian and Dominican institutions, triggered by means of the ICI, Brandimarte et al. [2] acquired rainfall data for the upper portion of the catchment, enabling the implementation of a quasi-distributed hydrological model (see e.g. [3]) for the comprehensive trans-boundary basin. Referring to topographic and morphological information provided by local authorities (e.g. land-use, soil-type variability and a coarse DEM for the whole river basin) the catchment was divided into 10 sub-catchments. Demanding to Brandimarte et al. [2] for more details on the reconstruction of the May 2004 flood event, Figure 4 summarizes the results of the hydrological analysis, providing the flow hydrographs at the catchment outlet (Jimanì) and at the confluences of the main tributaries of the River Soliette.

Flood mitigation plan for the River Soliette catchment

Referring to the extreme event of the 2004, Brandimarte et al. [2] proposed a rather complex compound of structural and non-structural measures that should be implemented at the catchment scale for the mitigation of the flood-risk. Since the heterogeneous hydrological and morphological characteristics of the upper and lower part of the basin, a comprehensive flood mitigation plan has to rely on several mitigation measures that must be implemented in a context of a wide and complete cooperation between Haiti and Dominican Republic. In fact, while fluvial erosion and impulsive sediment transport are the main issues affecting the mountainous part of the basin (the high river slope and wide deforestation favor soil erodibility), the lower part is characterized by gentler slopes that facilitate sediment deposition, generating alluvial deposits which may result on extended flooding. Concerning the lower portion of the basin, Brandimarte et al. [2] proposed a set of different measures, such as: masonry lengthwise embankments for flood restraint in proximity of urban areas of Jimanì and a series of non-structural measures which pursued flood-risk mitigation addressing the vulnerability of people and the adaptive capacity of the society (e.g. identification and delimitation of flood prone areas for controlling urban expansion, environmental education campaign for people leaving on floodable area and the implementation of a flood warning system).

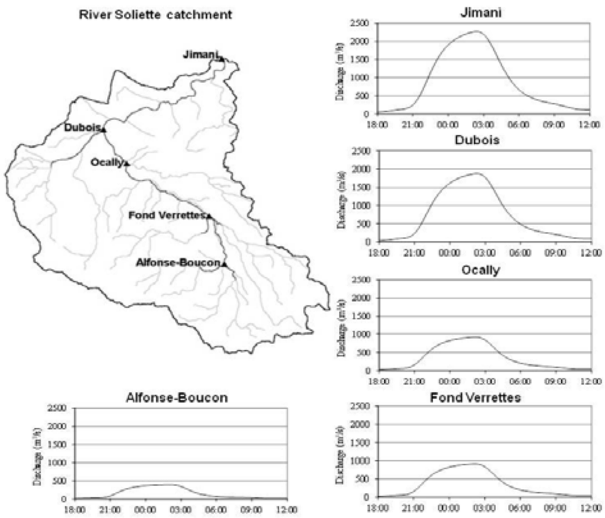

Fig. 4 - Sections of interest of the Soliette catchment with relative flow hydrographs reconstructed for the May 2004 event by means of a quasi-distributed hydrological model (see [2] for more details).

Concerning the lower portion of the basin, Brandimarte et al. [2] proposed a set of different measures, such as: masonry lengthwise embankments for flood restraint in proximity of urban areas of Jimanì and a series of non-structural measures which pursued flood-risk mitigation addressing the vulnerability of people and the adaptive capacity of the society (e.g. identification and delimitation of flood prone areas for controlling urban expansion, environmental education campaign for people leaving on floodable area and the implementation of a flood warning system). In relation with these measures, Figure 5 highlights the importance of institution and people awareness of hydraulic risk, showing how a large part of damages and fatalities occurred in 2004 could have been avoided in case of considering the flood hazard in the urban expansion plan.

Considering the upper Soliette basin, flood mitigation measures rely on a system of structural and non-structural measures, such as the strengthening of the pluvio-hydrometric gauging network (actually almost absent), the promotion of an environmental education campaign for the population living in the flood prone areas, the delineation of flood prone areas for controlling urban expansion and the promotion of a reforestation program in order to reduce the intense soil erosion and sediment transport observed during the 2004 flood event. In relation to this last problem, the most significant efforts planned in terms of structural flood-risk mitigation measures should be dedicated to sediment retain, ensuring the reduction of solid deposition in the lower part of the catchment. Starting from these outcomes, the present work took advantage of more extensive topographical surveys carried out on the upper part of the catchment, that were not available during previous studies, in order to further investigate flood mitigation measures along the River Soliette, evaluating in particular the opportunity and the benefits related to the implementation of a system of three “filtering” dams for retaining solid material.

HYDRAULIC-MODELING REQUIREMENTS AND OPERATIVE CONSTRAINTS

Next sections of the manuscript focus on the conflicting elements that characterized the evaluation of the feasibility of a system of three “slit” check dams in the upper part of the catchment: from one side the adverse operational condition in which we operated (limited economic and human resources and remoteness of the study area), and from the other side, the need to provide high resolution and accuracy topographic data for the implementation of a numerical hydraulic model along the upper part of the River Soliette.

Since the river appears single-channeled in the upper part of the basin we refer to a Preissmann Scheme one-dimensional (1-D) hydrodynamic model (see e.g. [6]) for which the topographic representation of the riverbed consists of a series of geo-referenced river cross-sections.

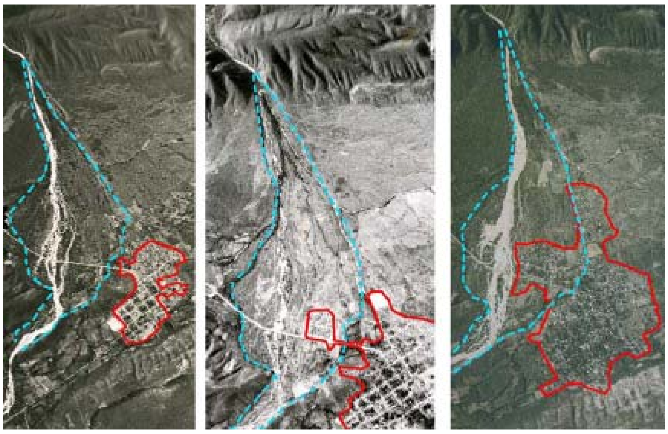

Fig. 5 - Urban extensions of Jimanì (Dominican Republic) in 1967, 1984, 2000 (areas delimited by red line from left to right) and May 2004 flood extent (dashed line).

The study river reach (of a length of ~7 km) was surveyed extracting several cross-sections with a relative distance of about 400 m, defining the cross-section width to ensure the survey of later banks 10 m above the river thalweg (see e.g. [7] and Figure 1). Furthermore, due to the necessity to design the system of check-dams, the hydraulic model required high resolution Digital Elevation Models (DEMs) for two different areas, pre-emptively identified during field trips as suitable for the construction of the filter dams (see red boxes in Figure 1). Concerning this last point, it is worth to highlight here that no geodetic infrastructure, mobile phone connection nor connections to the Geodetic Nationals Network were available in the study area. Instrumentation and surveying methods adopted in this case are discussed in the reminder of the manuscript.

TOPOGRAPHIC SURVEY

Technical constrains and limited founds available for the present study prevented from the use of sophisticated instrumentation (i.e. Airborne or Terrestrial Laser Scanning), while the best choice for this kind of survey was indentified in the GNSS (Global Navigation Satellites Systems) technique, whose receivers allow both the framing of the survey in an absolute geodetic and cartographic System and the detailed survey of sections and of digital elevation model (DEM) in selected areas. Since no vertices of a local geodetic frame were available in the area we defined the receiver position in an International Geodetic System (e.g. ITRS) by means of the Precise Point Positioning (PPP) approach which ensure high accurate absolute positioning using carrier phase observations acquired by geodetic GNSS receivers (see i.e. [8]). During the last years the improving of the satellite ephemeris precision, clock models, geophysical models, etc., have permitted a significant improvement of the PPP and nowadays, in case of at least 24 hours windows time observation, the overall accuracy appears comparable to others approaches based on double difference carrier phase data processing (see e.g. [9] and [10]). The final position in PPP is typically given in the same geodetic reference frame of the satellites orbits (IGS) and the transformation to the International Terrestrial Reference Frame (ITRF) is possible applying a daily seven-parameter transformation defined on the bases of orbits and clocks. The parameters of this transformation have been evaluated on a worldwide network (FLINN network) where, for each station, official coordinate in ITRF are well known, by means of the GISPY-OASIS II package, developed and maintained by JPL-NASA.

For what concern the detailed survey we adopted the Real Time Kinematic (RTK) technique both for the river sections surveys and DEM realization. In fact, this technique permits to estimate static or kinematic position of a receiver (Rover) in real time with respect a fixed reference station (Master), with an accuracy of few centimeters [9]-[11]. In our application the PPP survey provides precise coordinates in absolute ITRF2000 frame both for the Master and the Rovers positions. Usually the connection between master and rover receivers can be performed using or mobile or radio link. For this survey, since no mobile phone connections were available, we were forced to refer to VHF radio connection, which permits the possibility to send RTK corrections to many rover receivers simultaneously reducing significantly the time for survey.

In these constrained conditions the RTK technique provides some useful advantages. First of all, the surveyor can check on the screen, and in real time, the position of the receiver respect the coordinates of the reference station, with a centimeter level accuracy, and then navigate considering the requirement of the survey. Secondly, the connection with the master station permits a continuously data quality check that guarantee the final quality of the positioning also if a post processing is required. Concerning the precision of the RTK survey, many experiments are provided in the literature (see e.g. [12]-[14]), while others have been performed also by the authors ([15]), finding a precision in terms of planimetric and height components of few centimeters. In the light of all these considerations, the combination of PPP and RTK techniques constitutes the best approach in remote area, ensuring precision and accuracy which appear more than adequate for the type of survey that must be performed.

The survey was carried out using two different master stations along the valley, one located in the upper part the study area (see Figure 1), in the proximity of Fond Verrettes, and the second one located close to the bottom part, in the proximity of one of the two areas where the high detailed survey had to be performed (see boxes in Figure 1). The fixed coordinates of the two master stations were obtained by means of 20 minutes observation of code single point positioning, with an expected absolute accuracy of a meter. Adopting a sampling time of 1 second each GNSS receiver was set up both for a Real Time positioning and raw data (carrier phase and code) recording. Thanks to the precious logistical and training support offered by Haitian and Dominican Institutions the field survey was completed only in 3 working days, using in total 5 GNSS receiver available for the study.

Figure 6 reports some results of the topographic survey: raw data have been converted from a geodetic system into a cartographic projection (UTM, zone 18), while the points heights have been transformed from ellipsoidal to orthometric ones by using EGM96 geoid model and assuming the geoidal undulation as a constant for all the area. Detailed digital elevation models with a resolution of 1 meter required for the areas highlighted in Figure 1 (boxes) have been realized using kriging geostatistical interpolator, starting from the surveyed profile obtained as before described.

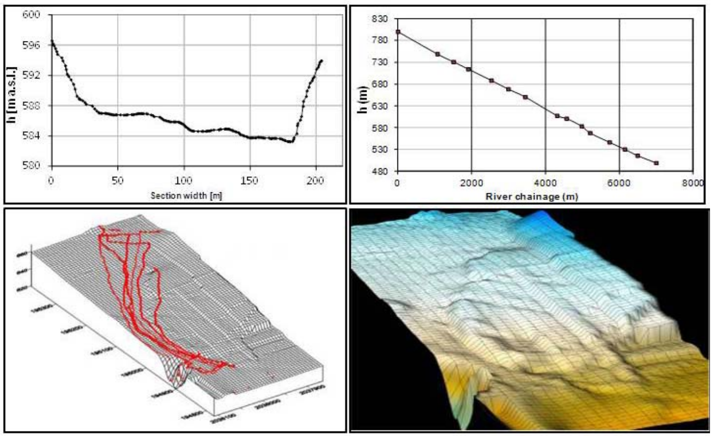

Fig. 6 - Results of the topographical survey: example of a river cross-section (up-left; see also traces on Figure 1), longitudinal profile of the upper part of the River Soliette (up-right), post-processed analysis with survey tracks and digital elevation representation of surveyed area (bottom panels).

HYDRAULIC ANALYSIS

Hydraulic modeling

Given the absence of a reliable data series relative to historical floods occurred over the study area (see also [2]) and considered the extreme intensity of the May 2004 event, we referred to it and, in particular, to the results of the hydrological analysis reproduced by Brandimarte et al. [2] (see also previous section) for the evaluation of flood-risk mitigation strategies along the River Soliette.

We referred to the collected set of topographical information for the implementation of a one-dimensional hydraulic model (1-D model) of the upper reach of River Soliette in order to deepen flood-risk mitigation strategies in the area of interest. In particular, Figure 1 shows the position of 15 cross-sections surveyed along the river, specifically along the stretch that goes from the urban area of Fond Verrettes to the confluence of River Ravine Dubois (left tributary relative to Dubois sub-basin). The 1-D model was built referring to the UNET code [16] that numerically solves the Saint Venant equations, through an algorithm that uses a classical implicit four-point finite difference scheme ([17]). The 1-D hydraulic model, once implemented and calibrated, represents a useful tool which ensure the possibility to investigate several fluvial geometric configurations, testing the efficiency and validity of different hydraulic structures in terms of flood-risk mitigation (see e.g. [18]-[20] for some example on the use of one-dimensional model).

The river geometry were reproduced referring to surveyed cross-sections which cover the overall study area (around 7 km reach of the River Soliette), while boxes on Figure 1 highlight the areas identified as suitable sites for the construction of hydraulic structures finalized to reduce the solid transport and for which two detailed DEMs were retrieved (see Figure 6). Thanks to the presence of detailed topographic models (DEMs), both the areas of interest were reproduced more precisely in the 1-D model by adding several additional river cross-sections extracted by means of

Geographic Information System tools. Due to the lack of observed hydrometric data for the model calibration, roughness coefficients adopted in the model were defined referring to typical values reported in the literature for river beds of similar characteristics (i.e. coarse sediments, pebbles and big boulders; [21]).

Flood-risk mitigation measures for the upper part of the River Soliette catchment

In order to reduce the flood hazard and flood exposure at the catchment scale it is necessary to envisage a comprehensive flood-risk mitigation plan composed of a series of different measures. Considering the upper part of the River Soliette, Brandimarte et al. [2] suggested the implementation of a series of non-structural measures, like for example the strengthening of the pluvio-hydrometric gauging network (actually almost totally absent), the delineation of flood prone areas for controlling urban expansion, the promotion of a reforestation program and the promotion of an environmental education campaign for the population living in the flood prone areas.

Among these, the problem related to the wild deforestation sounds particularly important in the light of significant problems related to sediment transport as observed during last major floods occurred in the area. In relation to this evidence, the most important efforts planned in terms of hydraulic infrastructures (structural measures) should be dedicated to the sediment retain, ensuring the reduction of solid deposition in the lower part of the catchment (i.e. alluvial fan near Jimaní, Dominican Republic) and avoiding the risk of flow levels rising that could originate floods on the urban area. In this context, the present work investigates the opportunity to implement a series of structural measures finalized to sediment retain in the upper part of the catchment. Referring to boxes reported in the Figure 1, the hydraulic analysis investigated the suitability of a system of three "filtering" dams (otherwise identified as " selective" or "slit" check dams). Figures 7 (upper panels) reports a detailed view of the areas identified as suitable for the dams, reporting also the traces of projected filter dams and additional cross-sections (yellow traces) extracted from detailed DEMs. The panel on the bottom left on Figure 7 reports the frontal view of one of the designed slit dams, while the panel on the bottom right highlights the results of the hydraulic simulation carried out over the study area.

This kind of dam is usually characterized by one or more narrow, vertical openings, going from the dam base up to the weir. The adoption of this structures appears the best solution for this case study because the sediment retain is obtained through the backwater effect induced by the structure, that makes possible the deposition of the sediments upstream the dam. Due to the nature of this structure and to the way it interacts with floods and sediments, its behavior appears customized to individual rivers and streams and their specific modalities of sediment transport. Final dimensions of projected dams and their interaction on flood propagation dynamics were investigated by means of the implemented 1-D model (see Figure 7).

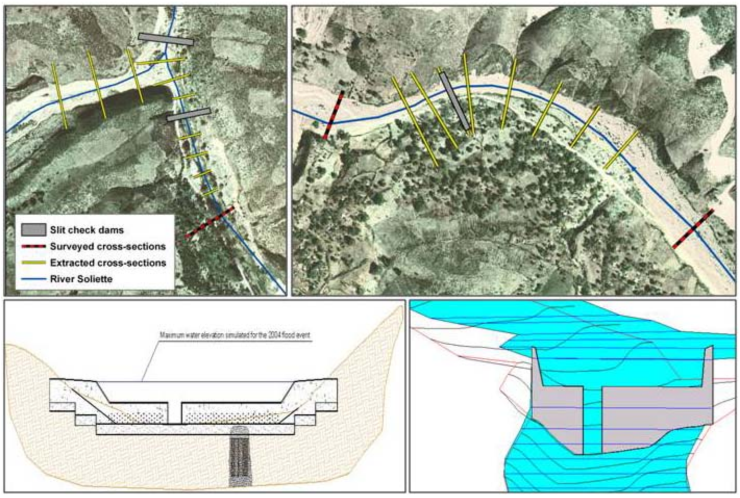

Fig. 7 - Position of designed check-dams for boxes a (upper left panel) and b (upper right panel) of Figure 1; bottom left: frontal view of a slit dam characterized by the vertical opening of about 5 m width; bottom right: three-dimensional view of the River Soliette as implemented in the 1-D hydraulic model.

FINAL CONSIDERATIONS AND REMARKS

The present paper summarizes the results obtained within the international cooperation initiative (ICI) for the development of a flood-risk mitigation plan for the River Soliette, a transboundary river that flows trough Haiti and Dominican Republic. Coordinated by the University of Bologna, the objectives of the ICI can be grouped as: a) institutional capacity building on flood-risk mitigation for local experts; b) hydrological and hydraulic analysis of the transnational River Soliette finalized to flood-risk mitigation. Triggered by the catastrophic consequences of the May 2004 flood event, the ICI promoted the collaboration between Haiti and Dominican Republic, enabling the cooperation of several technicians of the two countries in the field of flood-risk mitigation planning. The present paper briefly summarizes all the activities carried out during the cooperation which enable an enhanced characterization of the hydrological and hydraulic behavior of the trans-boundary river Soliette (see also [2]). In particular, the present paper mainly focuses on the topographic surveys and data analysis processes implemented on the upper-central stream of the river (Haitian part of the catchment). Referring to river cross-sections and detailed DEMs surveyed during several field trips we implemented a one-dimensional (1-D) hydraulic model for a ~7-km reach of the river. With reference to the May 2004 flood event occurred on the study area and reproduced by Brandimarte et al. [2], we used the 1-D model for the formulation of a suitable trans-boundary flood-risk mitigation plan, analyzing the effect of structural measures. The analysis highlighted how a flood-risk mitigation plan should be considered as a rather complex compound of structural and non-structural measures due to the hydrological and morphological heterogeneous characteristics of the study area.

Concerning the design of structural measures on the upper part of the river catchment, the numerical analysis mainly focuses on the efficiency of a system of three filtering dams adopted as measures for controlling the impulsive sediment-transport phenomena that occur during large flood events, among the main issues affecting the upper and central part of the catchment.

Furthermore, the ICI highlights the importance of an appropriate land-use planning and development as a fundamental step for flood-risk mitigation in this area, whose importance is enhanced by extreme poverty conditions which hamper the possibility of implement costly structural flood mitigation measure. Also, the generalized lack of hydrological and topographical data makes the design and implementation of reliable structural measures for flood-risk mitigations difficult: the absence of hydrological data prevents from a reliable estimation of expected flood event, while the absence of appropriate topographical data results on unreliable hydraulic analysis.

In these contexts, the opportunity to implement fast and reliable survey techniques such as those presented above appears of utmost importance, especially in the cases where global topographical datasets (i.e. Shuttle Radar Topography Mission-DEM; DEM-STRM) do not ensure the resolution and the accuracy required for reliable hydraulic investigations.

REFERENCE

[1] US Agency for International Development, Dominican Republic and Haiti – Floods. USAID/OFDA Fact Sheet #3, June, 2004.

[2] L. Brandimarte, A. Brath, A. Castellarin, G. Di Baldassarre, Isla Hispaniola: a trans-boundary flood risk mitigation plan. *Physics and Chemistry of the Earth,* Special Issue on Integrated water resources assessment, with special focus on developing countries, 34, 209-218, 2009.

[3] M.A. Smith, E.L. Harp, Flash flooding, debris flows, and hyperconcentrated water flows triggered by high-intensity rainfall of 23–24 May 2004 in south western Dominican Republic and south eastern Haiti, Site Assessment, July 16, US Geological Survey, 2004.

[4] INDRHI (Instituto Nacional de Recursos Hidraulicos), Inundaciones en Jimaní Rio Soliette, Diagnostico del Problema, Dominican Republic, 2004.

[5] CODIA (Colegio Dominicano de Ingenieros Aquitectos y Agrimensores), Informe técnico sobre desastre en Jimaní y soluciones propuestas. Capitulo de Riesgo, 2004.

[6] A. Preissmann, Propagation of translatory waves in channels and rivers, *Proc. First Congress of French Association for Computation*, pp. 433–442, 1961.

[7] A. Castellarin, G. Di Baldassarre, P.D. Bates, A. Brath, Optimal cross-section spacing in Preissmann scheme 1D hydrodynamic models, *J. Hydraul. Eng.*, ASCE 135 (2), 96–105, 2009.

[8] J.F. Zumberge, M.B. Helfin, D.C. Jefferson, M.M. Watkins, F.H. Webb, Precise point positioning for efficient and robust analysis of GNSS data from large networks, *Journal of Geophysical Research*, 102, 5005–5017, 1997.

[9] A. Hofmann-Wellenhof , H.E. Lichtenegger, J. Collins, GNSS: Theory and Practice (Fifth Revised Edition), New York, Springer-Verlag Wien, 2001.

[10] S. Gandolfi, L'approccio non differenziato (Precise Point Positioning) nel calcolo di posizioni mediante sistemi GNSS (in Italian), Bollettino SIFET (ISSN 1721-971X), 2009, 1, 121-137, 2009.

[11] C. Rizos, Network RTK research and implementation – A geodetic perspective, *Journal of Global Positioning Systems* 1(2),144-150, 2002.

[12] A. Pirti, N. Arslan, B. Deveci, O. Aydin, H. Erkaya, R.G. Hosbas, Real-Tıme Kınematıc GNSS for Cadastral Surveyıng, *Survey Review*, 41, 314 pp. 339–351, 2009.

[13] V. Janssen, T. Grinter, C. Roberts, Can RTK GNSS be used to improve Cadastral Infrastructure?, *Engineerıng Journal*, Volume 15 (1), Issn 0125-8281, 2011.

[14] M. S. Garrido, E. Giménez, M. C. Lacy, A.J. Gil, Testing precise positioning using RTK and NRTK corrections provided by MAC and VRS approaches in SE Spain, *Journal of Spatial Science*, Vol. 56, No. 2, 169–184 M. C., 2011.

[15] M. Barbarella, S. Gandolfi, E. Ronci, The Use of a GNSS Test Network for Real Time Application in Italy: First Results Based on Regional Field Test, *ION GNSS 19th International Technical Meeting of the Satellite Division*, 26-29 September 2006, Fort Worth, TX, USA, 1226-1232, 2006.

[16] R. L. Barkau, UNET One dimensional Unsteady Flow through a full network of open channels, US Army Corps of Engineerings, Hydrologic Engineering Center, Davis, 1997.
[17] A. Preissmann, Propagation of translatory waves in channels and rivers, *Proc. First Congress of French Association for Computation* (AFCAL), pp. 433- 442, 1961.
[18] A. Castellarin , A. Domeneghetti, A. Brath, Identifying robust large-scale flood risk mitigation strategies: a quasi-2D hydraulic model as a tool for the Po River, *Physics and Chemistry of the Earth*, Volume 36, Issues 7-8, pp. 299-308, 2011.
[19] A. Brath, A. Castellarin, G. Di Baldassarre, A. Domeneghetti, Linee strategiche di intervento per la mitigazione del rischio alluvionale lungo il corso medio-inferiore del Fiume Po (in Italian), *L'Acqua*, 2, pp. 9-24, ISSN 1125-1255, 2010.
[20] F. Pappenberger, K. Beven, M. Horritt, S. Blazkova, Uncertainty in the calibration of effective roughness parameters in HEC-RAS using inundation and downstream level observations, *Journal of Hydrology*, 302, 46–69, doi:10.1016/j.jhydrol.2004.06.036, 2005.
[21] V. T. Chow, Open-Channel Hydraulics, New York, USA, 1959.

UNMANNED AERIAL SYSTEMS FOR DATA ACQUISITIONS IN DISASTER MANAGEMENT APPLICATIONS

Irene AICARDI*, Filiberto CHIABRANDO*, Andrea LINGUA*, Francesca NOARDO*, Marco PIRAS*

*DIATI, Politecnico di Torino, Italy
e-mails: irene.aicardi@polito.it, filiberto.chiabrando@polito.it, andrea.lingua@polito.it, francesca.noardo@polito.it, marco.piras@polito.it

ABSTRACT

The potentiality of the Unmanned Aerial Vehicle (UAV) has already been proved by the military community, which has employed aircrafts without men on-board for reconnaissance missions and attack operations in the enemy field. The technological progress in the electronic and aerospace engineering fields allowed the development of low-cost UAVs characterized by a small size (mini-UAVs) and low weight, that can carry on-board imaging or non-imaging sensors. These advantageous features led the civil community to have an increasing interest in mini-UAVs. The excellent flight performances, the suitability for various types of missions, the inexpensiveness, and the capability to carry on-board different sensors, allow mini-UAVs to be employed in various missions. Nowadays, these systems allow to carry out missions in the following fields: land monitoring, remote sensing, agriculture and public security. Also the photogrammetric community has taken part to the research issues concerning the use of UAVs for map production.

The research group of Geomatics of the Politecnico di Torino has developed a set of interchangeable pods that can be mounted on a mini-UAV (a Hexacopter by Mikrokopter) devoted to emergency management in case of environmental disasters. This instrument is a low-cost mini-UAV equipped with photogrammetric sensors and capable of autonomous navigation (real time GNSS/IMU) and automatic digital image acquisition (characterized by a suitable geometric and radiometric quality). The platform is easily transportable on normal aircrafts and usable on the field, autonomously, by a couple of operators. The main innovation is to permits a real direct photogrammetric surveys in remote and disaster-affected areas in a short-range operative zone where it is not possible to carry out traditional photogrammetric flights. The acquisition technique allows the update of existing maps. Nevertheless, some test flights and practical applications have been performed in order to assess the autonomous flight performances and the suitability for photogrammetric flights.

INTRODUCTION

World disaster report - 2012 [1] suggests just how many lives have been and will be impacted by reported disasters in the decade 2002-2011 where “disaster” refers to all the events with a natural and/or technological trigger only, and do not include wars, conflict-related famines, diseases or epidemics:

- 7000 disasters in almost 10 years, including about 4000 natural disasters;
- 2684 million of people reported affected, 1.234 million of people reported killed, about the 93% for natural disasters;
- the estimated damage exceeds 1,450 billion euro of which more than 97% of natural disasters;
- the mortality rate increases and peaks after 48 h after the event are unlikely to survive beyond few weeks in the hospital.

The disaster management in emergency applications is always a race against time to move as fast as possible to reach all potential surveyors and yet move slowly enough to avoid creating additional collapse, damage or risk to rescuers and victims. The primary motivation is to save lives. Robots can assist in meeting this goal either by interacting directly with victims or structures or automatic support activities [2].

Advances in control engineering and material science made it possible to develop a particular type of robots: a mini or micro unmanned aerial vehicles (UAVs) equipped with cameras and sensors. The technology has a derivation from military applications; recently, however, products have also been of offered for the commercial market and have gained much attention, especially in some cheap products (e.g. Mikrokopter kit or similar). Having access to an aerial view over large areas is helpful in many applications, e.g., in disaster and law enforcement situations, where often only incomplete and inconsistent information is available to the rescue or police team. In such situations, airborne cameras and sensors are useful sources of informations which can help us to build an overview of the environment and to assess the current situation [3].

A conventional UAV can be regarded as an autonomous system that flies in the air, perceives the environment, and communicates with the ground station. It is typically controlled by a human operator using a remote control. More recent technology ([4]) is equipped with navigation sensors as Global Navigation Satellite System (GNSS) and Inertial Measurement Unit (IMU) to guide navigation using sophisticated on-board electronics that lead to a good stability in the air.

UAVs are valuable sources of information in many application domains such as environmental monitoring, surveillance and law enforcement, and disaster management [5]. Obviously, these application domains have different requirements and constraints regarding available resources, timing, etc. One important task for which UAVs are used is to provide a bird's eye view and thus allow to assess the current situation. Analysing different views, the image quality can be improved and even depth information can be computed, leading to a three-dimensional model of the environment.

The environmental monitoring requires the acquisition of high resolution and multispectral images and geometrical information of the environment, in different epochs. These data are then analysed to completely define the radiometric and 3D geometric characteristics of the interested area and the time evolution of described phenomenon. Accurate and high-resolution images taken from UAVs flying at low altitudes gives much more precise evidence compared to the pictures taken from helicopters or airplanes, thanks to the lower height of the flight. However, it is not necessary to automatically analyse the data and in real time. The Fly Planning of the drones and its optimizations can be prepared off-line. Data analysis is performed off-line after all the data have been acquired, using sophisticated and possibly time-consuming algorithms. The main motivation for using the UAVs is to cover the interested area by using less resources (time, energy, ...) and they are less intrusive compared to helicopters or airplanes.

Some specific examples may include forests monitoring, agriculture fields or snow terrains. Forests monitoring allows to observe the population of trees and their state as well as to estimate potential damages. In agriculture, UAVs can fly to observe crop growing or to document the damages after a thunderstorm. Analysis of the pictures acquired by the UAVs while flying over snow terrains can be used to estimate avalanche risks.

In disaster management, e.g., earthquake, flooding, wildfire [6], it is important to get a quick and correct overview of the situation since it is not possible to rely on available maps or imagery. Hence, similar to environmental monitoring, a first step is to employ a fleet of drones to map the affected area and thus provide a basis for planning further rescue activities. Additionally, sophisticated image analysis algorithms can be used on the UAVs to detect humans or certain objects and classify them.

The requirements in this application domain are much more stringent. First of all, one cannot rely on fixed infrastructure such as communication infrastructure, powerful central servers and power supply. Planning the mission off-line beforehand is not feasible. So mission planning has to be done on-line and the drones have to fly the calculated routes autonomously. The whole processing of aerial mapping has tight timing constraints; it is not possible to take the images and then employ sophisticated time-consuming algorithms for off-line image stitching. Detecting and classifying objects has to be done by the UAVs and thus requires considerable processing capabilities for real-time image analysis on-board the drones.

In this paper, the authors describe an example of UAV data acquisition and processing for a simulate emergency application. The test area where the simulation was carried out has been described and a detailed description of acquisition phase has been included. Data processing as well as the first results obtained by an automatic data processing that permitted the generation of an accurate digital terrain model (DTM) and an high resolution orthophoto useful to generate a Solid (True) OrthoPhoto (STOP) has been described. Finally some first conclusion are reported.

TEST SITE

In our study, the technology above described has been used over a stone quarry in Luserna S. Giovanni (Piedmont) (Fig. 1), which is a zone characterized by an important quarrying activity, several stone quarries and with important environmental impacts on the land.

Fig. 1 - The position of the stone quarry.

The quarry was recently closed by the administration because it was declared dangerous for instability and insecurity problems for which it was impossible to continue the extraction work.

The dismissed area has at one hand the landfill site for the material resulting of the extraction activity: this is an incongruent not-accessible hill that we can compare to a landslide to correctly simulate an emergency application. Moreover it was quite difficult to reach many areas of the site, and the reference points were barely recognizable from an ashore point of view, so that the possibility to realize a photogrammetric flight using UAV was extremely useful. In fact, the objective of the work was a survey to obtain a traditional representation such as an orthophoto and a 3D model of the area in order to verify the use of this techniques for the disaster management.

DATA ACQUISITION

The data acquisition methodology used in this case is similar to the traditional technique used in photogrammetry, using a small drone that allows to acquire aerial images of the site [7]. The aforementioned methodology was accompanied by a topographic survey employed for the determination of the coordinate of several 3D points of the quarry. The flight was previously planned using an existing map and a little scale satellite image, in order to establish the average elevation of the fly, the direction and the number of stripes.

All the acquisition operations have been completed in a few hours without a large number of operators (2 hours and 4 operators). This detail is very important as in emergency situations, which may be the instability of a quarry, it is essential to collect all the necessary data in the shortest possible time and subsequently to process them in the laboratory in order to clear the area as soon as possible.

According to the characteristics of the available data and the site, a map with scale 1: 100 has been chosen to conduct the analysis.

The topographic survey

Once on field, it was necessary to realize a topographic network in order to use the surveyed point as Ground Control Points (GCPs) or CPs (Control Points) in order to obtain the orientation of the photogrammetric block which could be realize using the UAV data.

In the test site (Figure 2a), 27 points (wooden markers) has been collocated in the area. They have been obviously positioned only on easily accessible sites: in this case, as could be the case of a landslide, not all the area was reachable, but it's sufficient to have some well distributed reference points, eventually integrated with natural ground points, to post-process the photograms Some targets were placed both on the ground, in order to be visible during the images acquisition step using the drone, and on the vertical wall behind the stone quarry.

Moreover two vertex as reference points (201 and 202) were used; these vertexes were measured with a GNSS instrumentation in static modality, in order to georeferencing this site. The markers' positions (Figure 2b) were measured from reference points using a total station (TS06 produced by Leica Geosystems).

(a) *(b)*

Fig. 2 - The GNSS vertices (red) and the surveyed points (green).

The total station measurements concerning the markers (the total station is an instrument that measures the horizontal angles (L_{sp}), the vertical angles (φ) and the slope distances (d_i)), were processed with the software GEOSW, that give back an .asc file and a .dxf file with the correct coordinates of the markers (Fig. 2-right).

At first, to immediately get a 3D model of the site, the coordinates of the markers were calculated using a local reference system and assigning the coordinates to the point of the total station (coordinates X_s=100,Y_s=100,Z_s=100).

However, a new georeferencing from the local reference system to global one (e.g. UTM-ETRS89 geodetic system) using the data obtained from the GNSS receiver is allowed and required.

The UAV image acquisitions

The aerial photogrammetry acquisition was carried out with a customized Hexakopter by Mikrokopter (Figure 3a), equipped with a digital camera, SONY-NEX 5 [8].

The flight plan elevation of the Hexacopter was set to about 50 meters and, for each flight, two adjacent stripes were acquired in order to obtain overlapped photogrammetric images of the whole stone quarry [9].

In order to maintain the control of the trajectories and the positions, the UAV was connected to a remote computer through an antenna (Figure 3b) (telemetry) and it can communicate with the software that send information about its position, orientation, height and speed. This telemetry allows the measurement and the recording of information between two remote devices in real time using a wireless communication (XBee).

In our case, the planned parameters of the UAV flight has been setting using Mikrokopter Tools: 2D waypoints positions in geographical coordinates, relative altitude with respect the height where UAV taking off the first time, speed for each path and compass direction during the flight (Figure 4). The UAV receives the flight instructions using telemetry and stores them on board to perform an autonomous flight. Anyway these parameter can be manually correct, during the flight, through a remote control, helping it to perform the flight in a correct way.

(a) *(b)*

Fig. 3 - The UAV (a) and the antenna used for the telemetry.

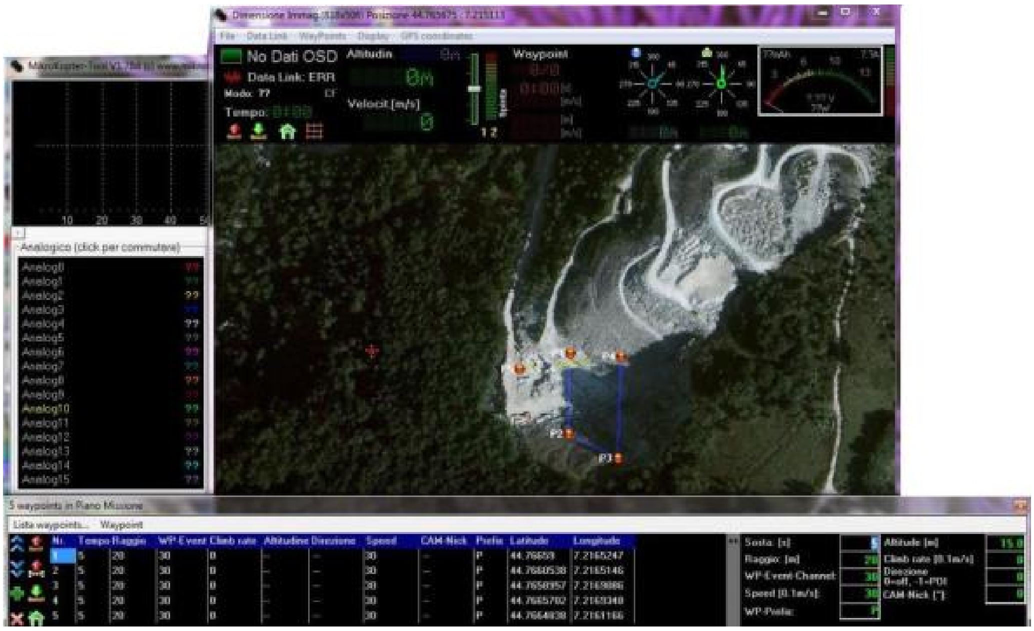

Fig. 4 - Planned waypoints for the 2nd flight on the Mikrokopter tools.

Two different flights has been realized, using in both cases four waypoints (Figure 5). One more flight was achieved with a different camera axis: normally it is oriented along nadir direction; in this flight the camera axis has been oriented in horizontal direction, in order to take photos of the rock face behind the stone quarry. This method is quite interesting because it can be used to take photos from heights that are difficult to reach in other ways.

During the survey, 1900 images were approximately captured in about 25 minutes of flight.

Fig. 5 – Trajectories of the two realized flights, as memorized by the incorporated GPS antenna of the UAV.

DATA PROCESSING

Once collected the material on the field, a post-processing on site using a notebook could be realized. In this case we simulated this phase in laboratory.

First of all, a small number of images has been chosen for each strip, to ensure a total coverage of the area and an overlap between images of about 60%. For data processing the software LPS (Leica Photogrammetric Suite) of ERDAS suite was employed. As usual the data processing steps are represented by two successive phases: internal orientation and external orientation [10].

The result of the photogrammetric process could be considered as a 3D model, eventually georeferenced in a suitable reference system, which can be used for the digital representation or to extract terrain models, orthophotos, or simply to make measurements.

According to the abovementioned steps, internal orientation was performed by considering the camera parameters: in this case a Sony Nex camera was used, whose calibration parameters were known and represent the input value of the software ERDAS to initialize a new project. In our case they are:

- pixel size: 5,21x 5,21µm;
- focal length: 15,5829 mm;
- principal point position: x_0= -0,0216 mm, y_0 =0,0364 mm.

After that, the external orientation was performed, by collimating corresponding points (GCPs) on each image and associating them with corresponding coordinates previously calculated in the local system [11].

The software allows to directly import the ASCII file of the coordinates and display them in the work screen, as it is shown in the red box in Fig. 6, so you can collimate the corresponding point on the images.

Point #	Point ID	>	Description	Type	Usage	Active	X Reference	Y Reference	Z Reference
1	1		1	Full	Control	✔	16.300	18.090	10.027
2	2		2	Full	Control	✔	17.119	14.971	10.370
3	3		3	Full	Control	✔	17.672	12.867	10.513
4	4	▶	4	Full	Control	✔	17.181	12.013	10.932
5	5		5	Full	Control	✔	14.124	11.202	10.648
6	7		7	Full	Control	✔	16.364	17.848	11.921
7	8		8	Full	Control	✔	17.159	14.814	12.493
8	9		9	Full	Control	✔	18.091	12.254	12.682

Fig. 6 - The points used for the external orientation with the reference coordinate in the local system.

In order to obtain the exterior orientation with sufficient redundancy, in each photo, should appear at least of 4

GCPs, although this number can change from each photogram.

When markers are not sufficient, supplementary points called Tie Points (TPs) are added, using natural references to have a better matching between the images. This is necessary in particular to involve inaccessible areas (present in the photos but, obviously, without markers) in the triangulation process. It is important that GCPs are well distributed, so that all the photograms participate in the triangulation (Figure 7).

It is possible to set some points (that exceed the minimum of 4 GCP for each photogram) as Control Points (CPs) which do not directly contribute to the triangulation process, but they are used to control the quality of the results. Moreover, it is possible to add other Tie Points (eventually automatically recognized by the software) with the aim of improving the quality of results and limit the deformations to have a better matching between the photograms.

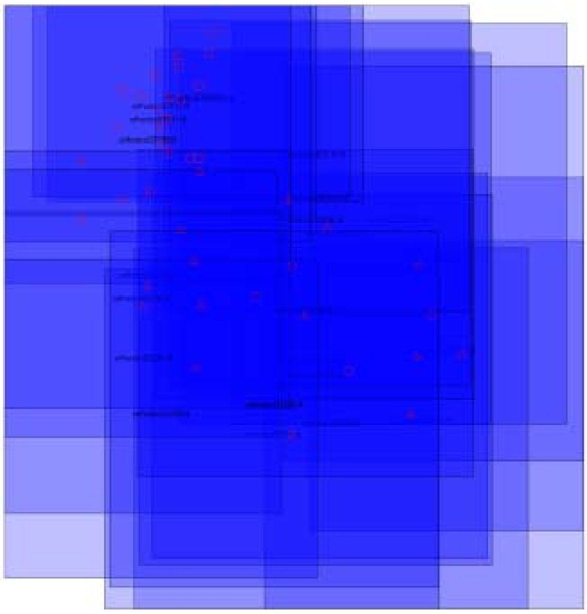

Fig. 7 - Triangulation of the frames used: the triangles are the control points and rectangles are the tie points.

If the first results of the Bundle Block Adjustment are not good, it is possible to delete or deactivate the points that have a big error and restart the triangulation process. For our purpose, according to the objective of the project we decide to consider only points that give an error lower than 20 centimetres in order to fit the admissible error relating with the scale of the final product.

In this way we can achieve a quite good product in a few time: the residual errors are restrained, very inferior to the admissible error (about 5 cm), and the processing time has been about 70 seconds for automatic photos matching and alignment (with an automatic research of control points), 2.5 minutes for constructing the DTM and 40 seconds for generate the textured solid model. So you can quickly have a useful base for researches and studies. With a bit more time you can also introduce known coordinates, in order to georeference the product.

RESULTS AND ANALYSIS

The software LPS can automatically process the DTM (Digital Terrain Model) of the specify area (Figure 8). It is an array of dimension values on the surface of the ground excluding the buildings, trees and other objects in the area. A 3D model is realized considering a discretization step equal to 20 cm [12].

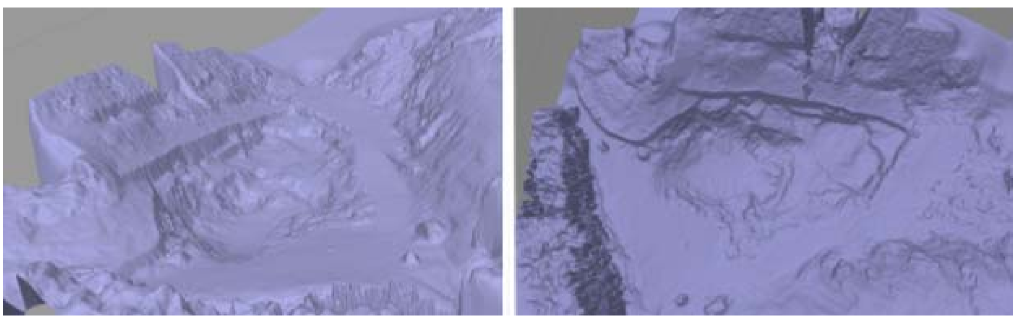

Fig. 8 - The DTM of the stone quarry.

The final step is to generate an orthophoto of the quarry.

The orthophoto is a cartographic representation in the form of digital georeferenced image: this corresponds to an orthogonal projection of the territory in the plan maps.

By using the ERDAS software, individual orthophotos were automatically realized after the BBA, which finally were merged in order to create the final mosaic. In the test site, PCI Geomatica were employed for the mosaic realization (Figure 9).

Fig. 8 - The orthophotos mosaic obtained after the triangulation.

Moreover using the achieved data it's possible to create a Solid (True) OrthoPhoto (Figure 10a, [13]), that is an image made by the fusion between a DTM, that contain the information about the height, and a orthophoto, that described the bidimensional representation. So, using appropriate software ("STOPviewer"), the 3D information could be read in an apparently bidimensional image (Figure 10b).

(a) *(b)*

Fig. 10 - The Solid OrthoPhoto generated (a) and an example of STOP viewer (b).

A specific software tool developed by the authors in Intel Visual Fortran language ("STOPGENerator") allows to make this product: you can first generate a single DTM of the whole area and then, using it, automatically generate single orthophotos associated with the DTM.

This processing has required 2 hours in order to generate the model and automatically extract the DTM and produce the orthophotos mosaic. For this processing a Lenovo S430 Laptop has been used (equipped with Windows8 professional, 64bit), employing an i7 IntelCore processor (speed 2,9GH) and a DDR3 8 GB Ram.

CONCLUSIONS

As it is reported in the paper, it is possible to say that the applied methodology is suitable for emergency situations such as the instability of a quarry, as it allows to acquire in a short time all the necessary data and obtain, with simple post processing, 2D and 3D measurable and georeferenced products that allow to study phenomena and plan the activities of recovery or restoration without the need to travel too much on the ground.

Therefore the use of the UAV can be considered adequate in all those situations in which the areas to be detected are hardly accessible or unstable, and there is the need to provide precise data in a short time.

Moreover, flying with an horizontal axis of the camera, we can easily reach different heights without physically move the operator. This can be very useful when emergency situations require it, both in natural and in anthropic context.

ACKNOWLEDGMENT

This project was carried out for a degree thesis and its realization was made possible thanks to funding from the PRIN 2010-2011, Research programs of national interest called "*Tecniche geomatiche innovative ed emergenti di rilievo, telerilevamento (da aereo, satellite, uav) e WEBGIS per la mappatura del rischio in tempo reale e la prevenzione del danno ambientale*" (person in charge: Prof. Santamaria, Università Partenope , Napoli). A special thanks to prof. Marilena Cardu for the proposal of the site and for her collaboration.

NOMENCLATURE

CP	Control Points
DTM	Digital Terrain Model
EO	External Orientation
GCP	Ground Control Point
GNSS	Global Navigation Satellite System
GPS	Global Positioning System
IO	Internal Orientation
IMU	Inertial Measurement Unit
LPS	Leica Photogrammetric Suite
TS	Total Station
TP	Tie Points
UAV	Unmanned Aerial Vehicle
E, N, Q	East, North, Geodetic Height
X_S, Y_S, Z_S	Coordinate of the point of the total station
h_S	Total station height
h_P	Prism height
d_I	Slope distance
φ	Zenith angle

BIBLIOGRAPHY

[1] M. Schmale, Under Secretary General, *International Federation of Red Cross and Red Crescent Societies: World Disaster Report*, Roger Zetter, 2012.
[2] R. Murphy, S. Tadokoro, D. Nardi, A. Jacoff, P. Fiorini, H. Choset, A. M. Erkmen, *Search and Rescue Robotics*. In: Handbook of Robotics. Springer, 1151–1173, 2008.
[3] M. Quaritsch, K. Kruggl, D. Wischounig-Strucl, S. Bhattacharya, M. Shah, B. Rinner, *Networked UAVs as aerial sensor network for disaster management applications,* Elektrotechnik und Informationstechnik 127(3):56-63, 2010.
[4] C. Coppa, A. Guarnieri, F. Pirotti, A. Vettore Accuracy enhancement of unmanned helicopter positioning with low cost system, Applied Geomatics 1 (3), 85-95, 2009.
[5] M. Quaritsch, E. Stojanovski, C. Bettstetter, G. Friedrich, H. Hellwagner, M. Hofbaur, M. Shah, B. Rinner, *Collaborative Microdrones: Applications and Research Challenges.* In: Proceedings of the Second International Conference on Autonomic Computing and Communication Systems (Autonomics 2008), Turin, Italy, 7, 2008.
[6] P. Boccardo, *New perspectives in emergency mapping*, European Journal of Remote Sensing - 2013, 46: 571-582, doi: 10.5721/EuJRS20134633, Received 30/05/2013, accepted 10/07/2013, 2013.
[7] H. Eisenbeiß, *UAV Photogrammetry*, Zurich, 2009.
[8] http://www.mikrokopter.de/ucwiki/en/HexaKopter.
[9] H. Eisenbeiss, A mini unmanned aerial vehicle (UAV): system overview and image acquisition, International Archives of Photogrammetry, Remote Sensing and Spatial Information Sciences, vol. XXXVI-5/W1, 2004.
[10] ASPRS, *Manual of photogrammetry*, 5th edition, 2004.
[11] K. Kraus, *Fotogrammetria I, Teoria e applicazioni*, Levrotto&Bella, 1994.
[12] O. W. Cheffins, *Accuracy of heighting from vertical photography obtained by helicopter*, London, England. The Photogrammetric Record, vol. VI No. 34, 1969.
[13] G. M. Forno, A. M. Lingua, S. Lorusso, G. Taddia, M. Piras, GSTOP: a new tool for 3D geomorphological survey and mapping, European Journal of Remote Sensing - 2013, 46: 234-249,doi: 10.5721/EuJRS20134613.